1-1-2007

Kinetic Studies of the Hydrolysis Reactions of Ruthenium (III) Complexes HIm trans-[$RuCl_4(im)_2$] and HInd Trans-[$RUCl_4(ind)_2$] by UV-Visible Spectrophotometry

Pramod K. Nangunuri

Kinetic studies of the hydrolysis reactions of ruthenium (III) complexes HIm trans-$[RuCl_4(im)_2]$ and HInd trans-$[RuCl_4(ind)_2]$ by UV-visible spectrophotometry.

By

Pramod K. Nangunuri

Thesis

to the Department of Chemistry

Eastern Michigan University

In partial fulfillment of the requirements

for the degree of

MASTER OF SCIENCE

in

Chemistry

December 2007

Ypsilanti, Michigan

DEDICATION

To

My Family,

Friends, and

Chemistry Department, EMU

ACKNOWLEDGEMENTS

I would like to thank my research advisor, Dr. Timothy Brewer; his interest, knowledge, dedication to this project, encouragement, and excellent guidance helped me in developing this project and thesis.

I am greatly thankful to Dr. Ross Nord and Dr. Vance Kennedy for accepting my proposal to serve on my thesis committee.

I would like to thank Dr. Krish Rengan for his wonderful guidance and support throughout my masters in the department.

Finally, I would like to thank all the professors in the chemistry department and staff, technical or non-technical members associated with the department, who helped me directly or indirectly during my study at Eastern Michigan University.

ABSTRACT

The ruthenium complexes have gained importance in cancer research in recent times, as several cancers have developed resistance towards platinum compounds. Platinum compounds have severe adverse effects that limited their use towards a wide range of tumors.

Ruthenium complexes are considered as pro-drugs, as they transform into anti-tumor active species in the body by hydrolysis, redox reactions, and reactions with biologically occurring nucleophiles. My project involved the synthesis of two ruthenium complexes with different ligands and the study of the hydrolysis reactions under different pH at room temperature using UV-visible spectrophotometry.

These studies will enable us to understand how structural factors and reaction conditions affect the kinetics, which may lead us to a better understanding of the stability and anticancer properties of these complexes. The data can also be used to conduct pharmacokinetic studies and in drug design.

My project presents the affect of different ligands and pH on the rate of hydrolysis of the ruthenium complexes. Imidazole and Indazole are the two ligands used for this study. We found that the hydrolysis reaction of the Ruthenium-Imidazole (RIM) complex is a two-step process that involved the formation of an intermediate. The rate constants for the two steps in the reaction were determined and found to follow first order kinetics. The rate hydrolysis of the RIM complex in water at room temperature was found to be greater at pH 8.4 for the first complex. The hydrolysis of the RIM complex was found to be independent of basic pH.

The hydrolysis reaction was found to be 10 times faster with indazole as a ligand than with imidazole as a ligand. The RIM complex is more stable than the Ruthenium-Indazole (RIN) complex. It was found that as the basicity of the ligand decreases, the hydrolysis rate increases and stability decreases. As the pH increased, the hydrolysis rate increased for RIN complex. The hydrolysis of RIN was observed to be very fast at higher pH levels.

The reaction order and kinetic rate constants for hydrolysis of RIN complex were not estimated quantitatively because the hydrolysis involves a complex process with multiple steps or different pathways at higher pH. The hydrolysis curve did not retain its signature shape at higher pH for the RIN complex. Future studies of the hydrolysis products of the RIN complex obtained at different time intervals with HPLC and NMR spectroscopy may reveal the actual mechanism of hydrolysis or the steps and pathways involved in the hydrolysis process. This may help us in establishing the kinetic data.

TABLE OF CONTENTS

LIST OF TABLES

Table

LIST OF FIGURES

Figure

CHAPTER 1: Introduction

Trans-imidazolium(bisimidazole) tetrachlororuthenate(III) {HIm trans-[$RuCl_4(im)_2$]}, or RIM, and trans-indazolium(bisindazole) tetrachlororuthenate(III) {HIn trans-[$RuCl_4(ind)_2$]}, or RIN, are two promising anticancer ruthenium complexes that are in phase I clinical trials.[1,2] Their interaction with biological molecules is also established by various groups of scientists. [2,3,4,5] Ruthenium complexes have advantages like reduced toxicity, novel mechanism of action, prospect of non-cross resistance, and a different spectrum of activity when compared with anti-tumor platinum (II) complexes currently used in the clinic.[6]

Presently only a few studies exist on the hydrolysis profiles of anti tumor ruthenium (III) complexes under different pH conditions.[7, 8] None of them concentrated on the rate constants of the reaction or on the reaction order. We attempted to understand the order of reaction and rate constants for the hydrolysis reaction of two ruthenium complexes with different ligands (Imidazole and Indazole) under different pH conditions (4.2 to 9.4) at room temperature. The following section gives information about cancer, hydrolysis, and importance of the kinetics in hydrolysis reactions of these ruthenium complexes in the cancer study.

1.1 Cancer

Uncontrolled and unregulated growth of cells, from sequential acquisition of somatic mutations in genes that control cell growth, differentiation, and apoptosis, or that maintains genomic integrity, is called cancer. Mutations can be produced by environmental mutagens such as chemical carcinogens or radiation. Cancer is also referred to as malignant tumors or malignant neoplasia.[9]

The characteristics of malignant neoplasm cells are irregular shape, non-cohesiveness, and invasion of their surroundings in a destructive fashion. Another dangerous property of malignant neoplasm is referred to as metastasis, in which the cancer cells spread randomly. They separate from the parent tumor and enter the circulatory system, float elsewhere, and are able to extravagate, continue their proliferation, form a secondary locus of tumor, and so on.[10]

1.1.1 Types of Cancer:

The following classification is based on the point of origin of the cancerous tumor in the body:

Carcinoma- Cancer that begins in the skin or in tissues that line or cover internal organs.

Sarcoma- Cancer that begins in bone cartilage, fat muscle, blood vessels, or other connective tissues or supportive tissues.

Leukemia- Cancer that originates in blood-forming tissue like bone marrow.

Lymphoma and myeloma- Cancer that originates in the cells of the immune system.

Central nervous system cancer- Cancer that begins in the tissues of brain and spinal cord.[11]

Cancer is the second leading cause of death in United States; half of all men and one third of all women will develop cancer during their lifetimes.[12]

1.1.2 Drugs available for treating the cancer

Platinum compounds like cisplatin and carboplatin are widely used cancer drugs for treating ovarian, testicular, lung, and neurologic cancer. Damage of DNA has been proposed as the mechanism of action of these drugs in controlling the cancer cells.[13, 14, 15, 16]

Development of resistance, adverse effects like nephrotoxicity, loss of hearing, loss of sensation on skin, solubility problems, and expensive cost are limiting the use of these platinum drugs.[6, 17]

Fluorouracil and methotrexates are antimetabolites used for treating cancers of the colon, rectum, breast, stomach, and lung. These cancer drugs prevent the synthesis of DNA by preventing precursors necessary for DNA synthesis. They substitute themselves in the DNA, causing damage to it, and thus prevent the growth of tumor cells. Damage to liver, lungs, and kidneys are severe side effects of these cancer drugs, and application of these drugs in cancer treatment has been decreased because of the severe side effects.[18] Many drugs are available for treating cancer, but these are the two main classes of drugs widely used to treat cancer associated with lungs, brain, gastrointestinal tract, and reproductive organs.

1.2 Ruthenium

Ruthenium is a polyvalent metal with atomic number 44 belonging to the transition metal group. Metal complexes made of ruthenium are presently in focus for cancer research as they are showing promising results in controlling types of cancer models in vivo, along with colorectal carcinoma of rats. Chemical properties such as rate of ligand exchange, range of accessible oxidations states, and ability of ruthenium to mimic iron in binding to certain biological molecules make these compounds well suited for medical applications as an alternative to conventional antitumor drugs in the treatment of cancer. There are fewer solubility problems with ruthenium complexes.[6]

The kinetic stability of ruthenium in different oxidation states, the often reversible nature of its redox couples, and the relative ease with which mixed -ligand complexes can be

prepared by controllable stepwise methods makes ruthenium complexes the focus of cancer studies. Most of the ruthenium complexes tested for antitumor activity have shown less cytotoxicity than conventional drugs available for treating cancer. Cancer cells secrete lactic acid, which decreases the pH of the environment around cancer cells. The supply of oxygen also decreases around the cancer tumors. An environment with lower oxygen and pH favors the reduction of Ru (III) to the more reactive Ru (II) (active drug) oxidation state, which provides selective toxicity to the tumors only.[19] It was observed that the ruthenium complexes inhibit the DNA synthesis for controlling the antitumor activity.[20, 21, 22]

1.2.1 Structures of ruthenium complexes used for the study

Trans-imidazolium(bisimidazole)tetrachlororuthenate(III){HImtrans-[$RuCl_4(im)_2$]}, or RIM, shown in Figure 1.2-1, and trans-indazolium(bisindazole)tetrachlororuthenate(III) {HIntrans-[$RuCl_4(ind)_2$]}, or RIN, shown in Figure 1.2-2, are two promising anticancer ruthenium complexes that have passed the phase I clinical trials. In the first complex, a ruthenium atom is coordinated to two imidazole ligands and is also bonded to 4 chloride atoms. In the second complex, two indazole ligands are coordinated to ruthenium and 4 chloride atoms. Both the complexes have shown significant anticancer activity against the walker 256 carcinoma, MAC 15A colon tumor, B16 melanoma, solid sarcoma 180, and chemically induced colorectal adenocarcinoma of rats.[19]

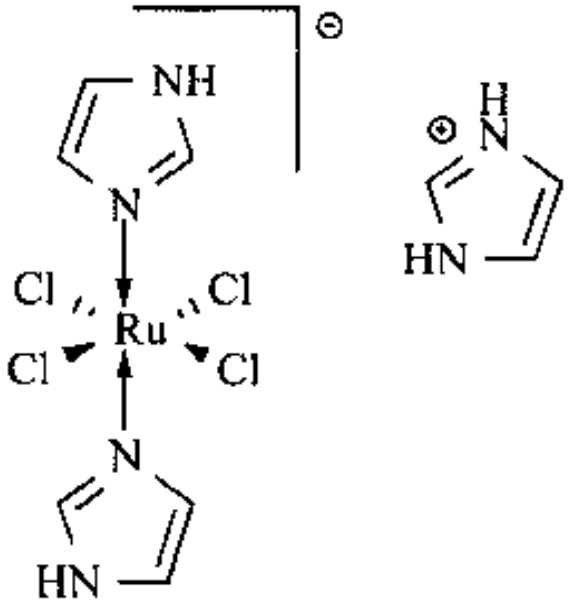

Figure 1.2-1 Chemical structure of HIm trans-[$RuCl_4$ $(im)_2$].

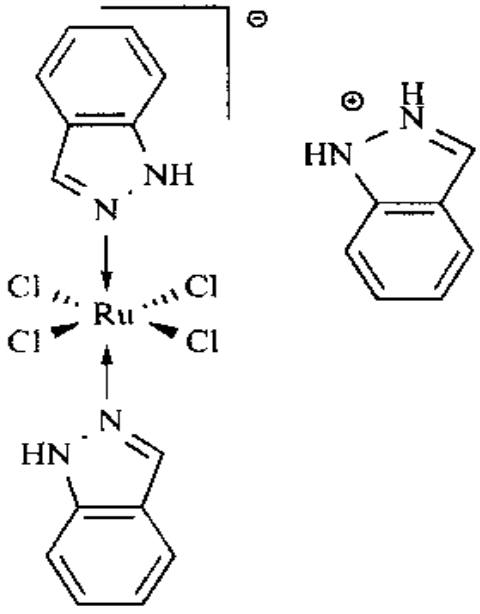

Figure 1.2-2. Chemical structure of HInd trans-[$RuCl_4$ $(ind)_2$].

1.3 UV-visible spectrophotometry

UV-Visible spectrophotometry is well suited for monitoring the reactions of substances with a chromophore. Reactions like hydrolysis, in which a chloro ligand of the

ruthenium complex is replaced by a water molecule, can be followed by this method. The hydrolysis of ruthenium-chloro complexes can be followed at wavelengths corresponding to the ligand-field spectrum of the chromophore. The hydrolysis rate constants of cisplatin and related complexed, anticancer drugs were explored using UV-spectrophotometry.[13, 23, 24]

The basic principle in the working of UV-visible spectrophotometer is the linear relationship between the concentration and absorption. The concentration of an absorbing analyte is given by Beer's law:

$$A = \epsilon bc \qquad 1.3\text{-}1$$

Where A is absorbance, b is the path length, c is the concentration, and ϵ is the absorptivity coefficient, which is a measure of amount of light absorbed per unit of concentration, it is constant for a particular substance at a particular wavelength. The sample solution (concentration, c) to be analyzed is placed in a cell (with a specific path length, b) and light from the source (a hydrogen or deuterium lamp for the ultraviolet region and a tungsten or halogen lamp for the visible region) is passed through it and also through the reference cell, which has only solvent, simultaneously. The spectrophotometer compares the light passing through the sample and reference solutions, and the transmitted radiation is detected by a detector. By scanning over a range of wavelength (200nm-700nm) of the light passing through the cells, the amplified signals are recorded in the form of an absorption spectrum. The concentration of the unknown can be calculated by using the absorbance measured (A), the known values of the absorptivity coefficient and the path length.[25]

When the light is absorbed by the valence electrons (present in the σ, π, and non-bonding orbitals) of an atom they excite to a higher energy level (σ^*, π^*orbitals) from the

ground level, and since these levels have fixed energies, the peaks obtained in the spectrum correspond to these transitions.

Figure 1.3-1 is the schematic representation of the single beam UV-visible spectrophotometer in which the source of light, mirrors, reference cell, sample cell, detector, and recorder are represented.

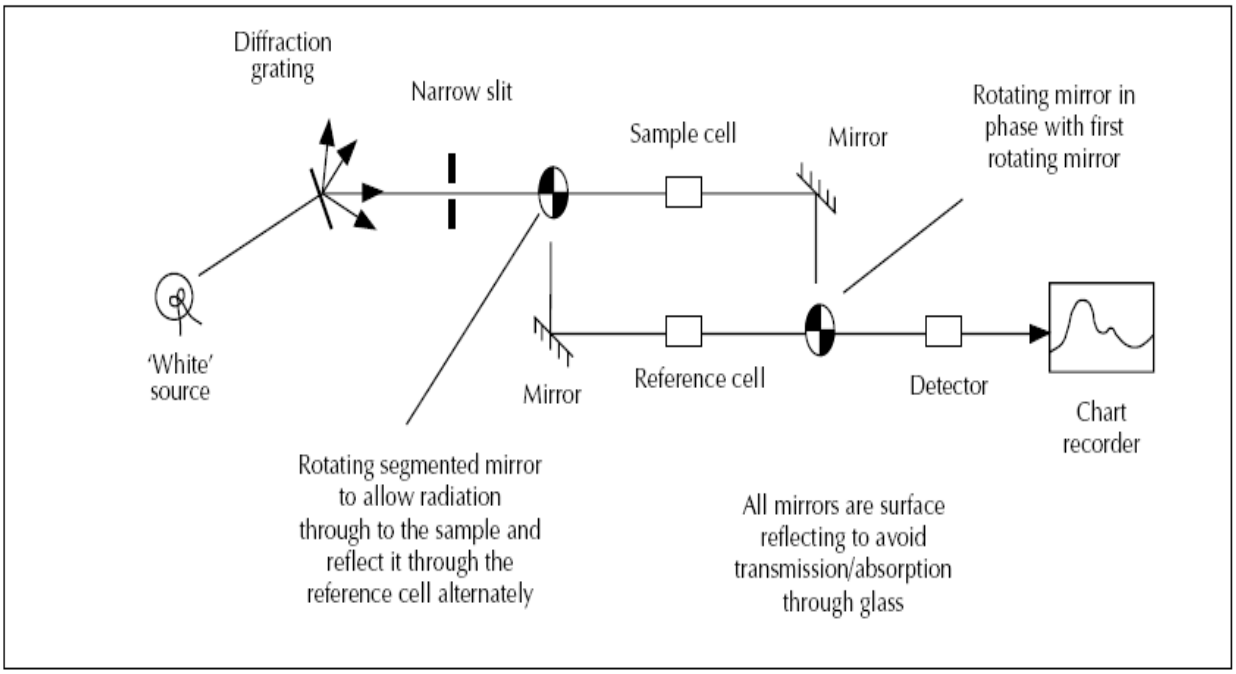

Figure 1.3-1. Schematic representation of the working of UV-visible spectrophotometer. (http://www.chemsoc.org/pdf/LearnNet/rsc/UV_txt.pdf).

1.4 Hydrolysis

Hydrolysis reactions are of many types, but the basic hydrolysis reaction is one in which the hydroxyl group of the water molecule or the water molecule itself gets substituted on the reactant. It is also a double displacement reaction and it is a reversible process.

1.5 Kinetics of hydrolysis reaction and its importance in the cancer study.

The study of reaction rate is called kinetics. It is studied by measuring the change in the quantity of either mass or volume or concentration per unit time. In this project, the change in the concentration is measured on par with time. The pro-drug, which is in an inactive form, transforms to an active drug by hydrolysis. The time taken for the pro-drug to transform to an active drug is important in a cancer study because the rate determines the duration of action or time required to cure the fast growing cancer cells or time required to control the rapidly dividing tumor cells. This also completes with the clearance rate for the compounds.[7]

The study also helps in the design of new drugs because the rate of ligand exchange can be studied in these reactions, which aids in understanding the activity, selectivity, and reduced side effects. The drug dosage also can be calculated using these kinetic studies.

Kinetic study of the hydrolysis reaction of ruthenium complexes gained importance after researchers started looking for alternatives to the conventional anti-tumor drugs used in the treatment of cancer. Ruthenium complexes act as pro-drugs before injection into the body and change their coordination when reacting with bio-molecules in executing therapeutic action.[7] Such changes may involve ligand substitution, redox processes, and formation of aqua complexes. The conditions that effect the coordination are important because the knowledge gives us some insight into the stability and storage of the anticancer drugs. The data obtained can be extrapolated to understand the clinical applications and further reactions of the drugs in blood and cells.[19]

Many water soluble ruthenium complexes, especially ruthenium(III) complexes of the general formula $HL(RuCl_4L_2)$ with two trans-bonding heterocyclic ligands L bound to ruthenium via nitrogen, show good antitumor activity in different tumor models. The first

reaction step of interest is hydrolysis because aquation has proven to be an important step in the activation of cisplatin, the metallic anti-cancer drug that was discovered first and is the most widely used drug to treat cancer, and aqua complexes are generally orders of magnitude more labile than the corresponding chloro complexes.[8]

Hydrolysis reaction

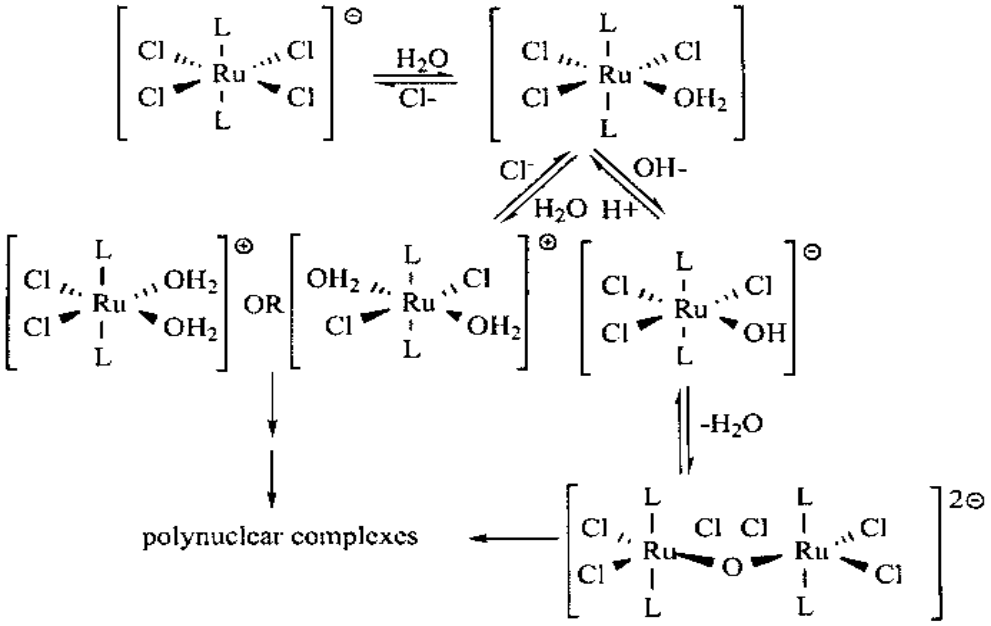

Figure 1.5-1. Possible Hydrolysis pathways of ruthenium complex anion trans-[$RuCl_4L_2$].

Figure 1.5-1 shows the possible pathways in hydrolysis reactions and the decomposition compounds of the complex anion trans-[$RuCl_4$ (ind) $_2$] or trans-[$RuCl_4$ (im) $_2$]. It is assumed that in the first step, one of the chloride ligands gets substituted with water and then another chloride is replaced in the second step. After this, the ruthenium complex with two chlorides, two water molecules, and two ligands join together to form poly nuclear complexes, which bind to the corresponding nucleotides on DNA and execute their toxic effect.

NAMI-A, imidazolium trans-tetrachloro (dimethylsulfoxide) imidazoleruthenium (III) $H_2Im[trans\text{-}RuCl_4(DMSO)HIm]$, a ruthenium complex, which is in Phase I clinical trials of a cancer study, was investigated by Bouma et al. for its chemical stability. The degradation of NAMI-A consisted of stepwise hydrolysis of the chloride ligands, in acidic media accompanied by hydrolysis of the DMSO group, followed by formation of poly-oxo species. It has been suggested there could be two transformations in the compound. One transformation, which is in the early stages of degradation (substitution of ligands), depends on the pH of the buffer solution, and the next transformation could be caused by further substitution of ligands, polymerization, or reduction of the chromophore Ru (III). Degradation of NAMI-A followed (pseudo) first order kinetics at pH values < 6 and zero-order kinetics at pH values ≥ 6. The solution is most stable in the pH region 3-4. Using the data, they concluded that an acidic solvent should be used for NAMI-A administration during the clinical trials.[26, 27, 28]

The first two steps in the hydrolysis process of NAMI-A were proved by Chen et al., theoretically using a computational method, density functional theory (DFT). A comprehensive study has shown the structures involved in the first two steps of the hydrolysis process, and the rate constants for the two steps were determined and were in agreement with the experimental values. Detailed energy profiles for the reaction steps concluded that the solvent effect plays an important role in the hydrolysis of NAMI-A apart from the buffers used.[29]

Stability of a ruthenium (III) complex, 2-Aminothiazolium [trans-tetrachlorobis (2-aminothiazole) ruthenate (III)], was studied by Mura et al. in different solutions. and the hydrolysis was studied in aqueous solution at different pH values. Studies proved that

increasing the basicity of the nitrogen heterocyclic ligand in the ruthenium complex increases the rate of hydrolysis. The increase of electron transfer from the nitrogen to the metal in the ruthenium complex increases the dechlorination.[30, 31, 32]

Studies on hydrolysis reactions of ruthenium complexes by different groups of researchers found the following three important results. Messori et al. found that Ru-thiazole complexes hydrolyse faster at pH 7.4, and the replacement of imidazole by less basic thiazole did not significantly affect the kinetics of the chloride release.[33] The secondary ligand stabilizes the ruthenium (III) cation so that the metal ion is not delivered to the tissues during transportation, nor does it undergo hydrolysis /oxidation/reduction processes until it reaches the final target. It also increases the solubility in water and/or facilitates intracellular transit of the metal; this was proven by Vilchez et al.[34] The UV and HPLC studies of the hydrolysis reactions in physiological buffer showed that the imidazole complex is much more stable than the corresponding indazole compound. The two complexes were first studied in these papers by Keppler et al.[35, 36]

The hydrolysis of NAMI in presence of Bovine Serum Albumin at 25^{o}C in phosphate buffer was analyzed spectrophotometrically by Messori et al. It was found that hydrolysis proceeds through two very distinct steps; first, the decrease of the characteristic band at 400nm and the concomitant increase of a band of similar intensity at 346nm are observed. Second, the progressive decrease of the latter band takes place. This corresponds to the sequential replacements of the two ruthenium-coordinated chloride groups by hydrolysis.[37] Kratz et al. stated that the loss of two coordinated chlorides is the prerequisite for any further reactivity.[38]

The hydrolysis of the complex trans-tetrachlorobis (indazole)ruthenate(III) was studied by Pieper et al. in different solvents by UV-visible spectroscopy and NMR using different buffer systems. The solvolysis of the complex in organic solvents or aqueous mixtures of ethanol, acetonitrile, and DMSO gave one main product, but hydrolysis in water or buffered solutions gave many products in different steps. The formation of the neutral monoaqua complex was observed in the hydrolysis of the ruthenium complex in all the solvent systems, even in the unbuffered solvents. The formation of hydroxo complexes, and then further reaction with di- or polynuclear hydroxo or oxo-bridged complexes, was found to be accelerated at higher pH and thus it was concluded that hydrolysis of the ruthenium complex is strongly pH dependent. The NMR studies of the hydrolysis gave limited results because of the paramagnetic ruthenium metal.[39]

1.6 Research goal

The goal of my research is to study the effect of different ligands (L=imidazole, indazole) on the hydrolysis process of ruthenium (III) complexes of the general formula $HL(RuCl_4L_2)$ at different pH values and room temperature. Another goal is to estimate the stability of the complexes trans-imidazolium(bisimidazole)tetrachlororuthenate(III) {Him trans-$[RuCl_4(im)_2]$} and trans-indazolium(bisindazole)tetrachlororuthenate(III) {Him trans-$[RuCl_4(ind)_2]$}. This study will also focus on the determination of the kinetic order of the reactions and their rate constants.

CHAPTER 2: Experimental

2.1 Instrumentation

A Perkin Elmer Lambda 20 (UV-visible spectrophotometer) with hydrogen and deuterium lamps as the source of UV and visible lights was used to measure the absorbance of all the samples. The instrument was also associated with a temperature controller, which maintained the temperature (around 23^{o}C) throughout the kinetic studies. The kinetics of the hydrolysis reaction was studied using the same instrument by monitoring the absorbance change at a constant wavelength for the reaction. Hanna instrument 8417 (pH meter) was used to measure the pH of all the buffers.

2.2 Materials

Ruthenium (III) chloride hydrate (reagent plus, Sigma Aldrich), imidazole (99%, Aldrich), and indazole (98%, Aldrich) were used for the preparation of two ruthenium complexes. Sodium phosphate monobasic ($NaH_2PO_4 \cdot H_2O$) [Analytical reagent, Mallinckrodt] and sodium chloride crystal salt (NaCl) [Certified A.C.S, Fischer] were used for the preparation of buffers.

Synthesis of HIm trans-[$RuCl_4$ (im) $_2$]: 1 gm of $RuCl_3$ was dissolved in a mixture of 25 mL of ethanol and 25 mL of 1N HCl. The mixture was refluxed for about 3 hrs, solution was evaporated to 9 mL, and 1N HCl was added to give a total volume of 12 mL. Ten mL of this ruthenium solution was added to a suspension of 2.0 gm of imidazole in 1mL of 6N HCl, and the solution was cooled in ice for two hours and then allowed to stand for 2 days at room temperature. Then large brownish red crystals were filtered off, washed with water/ethanol, and dried under vacuum.[40] The synthesis equation of ruthenium-imidazole is represented in Figure 2.2-1.

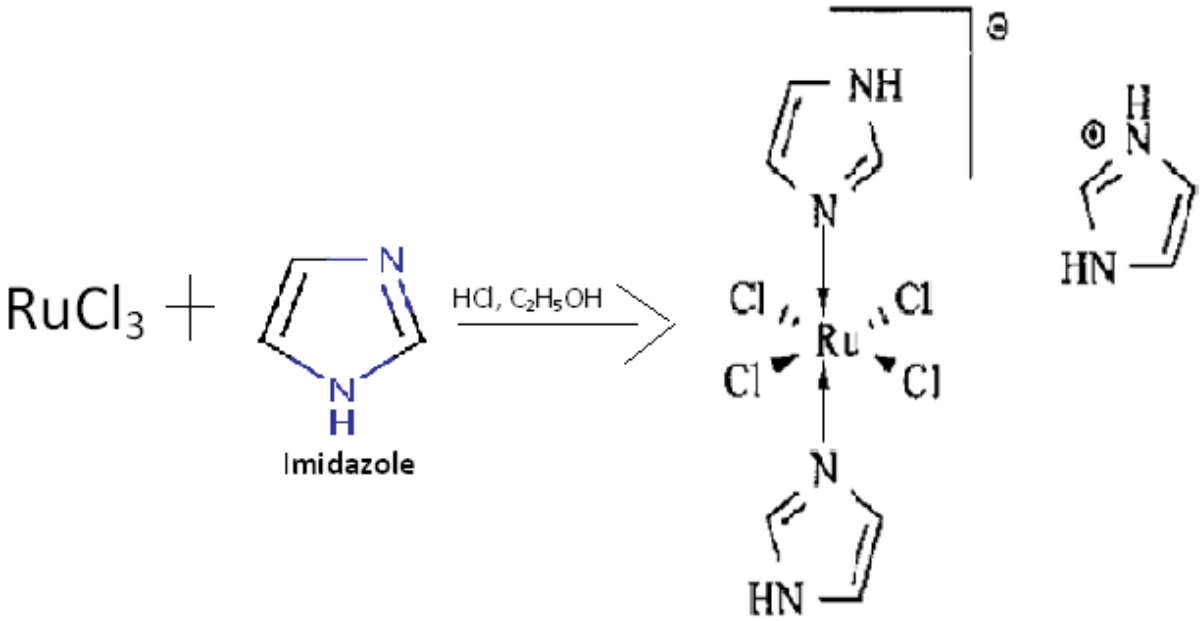

Figure 2.2-1 Synthesis of Ruthenium-Imidazole complex.

Synthesis of HInd trans-[$RuCl_4$ (ind) $_2$]: 0.8 gm of $RuCl_3$ was refluxed for 1hr in a mixture of 5 mL of 1N HCl and 5 mL of ethanol. Then the dark red solution was cooled down to 40^{o}C, and the alcohol from the solution was removed by heating. The residue obtained was filtered and filled up to 10 mL with 1N HCl. Two mL of this ruthenium solution was added

to a hot solution of 0.6 gm of indazole dissolved in 8 mL of 12N HCl at 70^{o}C. The mixture was stirred and heated for about 15 minutes at 80-90^{o}C. Ochre (brownish orange) colored solid separated from the solution almost immediately. Stirring was continued until ambient temperature was reached and then the crude material was separated and stirred again for 2 hrs at about 80-90^{0}C to remove the HCl residues. Then the solid was filtered and washed with ethanol and diethyl ether and dried in vaccum.[41] Synthesis of ruthenium-indazole complex is represented in Figure 2.2-2.

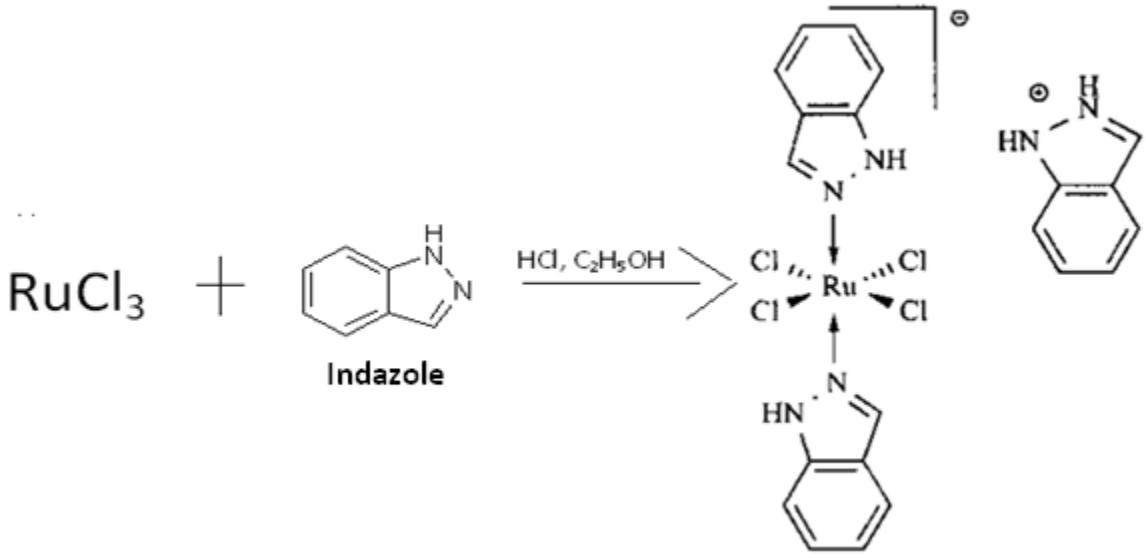

Figure 2.2-2 Synthesis of Ruthenium-Indazole complex.

Phosphate buffer: Buffers of pH 4.2, 5.4, 6.4, 7.4, 8.4, and 9.4 were prepared by using sodium phosphate (NaH_2PO_4 50mM) and sodium chloride (NaCl 100mM) in deionized water. 1M NaOH solution was used to make up the pH of the buffers accordingly.

2.3 Method

Compounds to be analyzed were dissolved (not a quantitative study) in the freshly prepared buffer, and absorbance readings were recorded before and after the kinetic study over the wavelength range of 200nm to 700nm, using the UV-visible spectrophotometer. The

kinetics of the hydrolysis reaction was studied at definite wavelengths (400nm for RIM and 287nm for RIN) for a certain period of time at room temperature in different buffers.

Concentrations between 0.005 and 0.2 M (for both RIM and RIN) were used to study the hydrolysis reaction. So the ratio of the ruthenium complex to water is approx. 1:1000 or more. The reactants, water and ruthenium complex, react such that the product formation is mostly dependent on only one reactant, the concentration of ruthenium complex, whereas the change in the water concentration is very much less and negligible.

Hydrolysis studies were conducted for 5 hrs, 6 hrs, 9 hrs, 10 hrs, 12 hrs and 24 hrs (for the reactions of RIM complex) and 15 minutes, 30 minutes, 1 hr, 2 hrs and 6 hrs (for the reactions of RIN complex), at all the buffer levels (pH=4.2, 6.4, 7.4, 8.4, and 9.4) at room temperature (around 25^0C). Each buffered sample was studied for at least three different periods of time, and the average of those rate constants obtained for three trials was determined.

Kinetic data were analyzed using the Vernier software Graphical Analysis program. The program allowed for the fit of a multi-parameter curve based on pseudo-first order kinetics and more complicated curves such as a two-step hydrolysis that has been proposed for these reactions.

CHAPTER 3: Results and Discussion

3.1 Ruthenium-Imidazole complex (RIM)

In the absorbance spectrum of RIM (sample spectrum, Figure 3.1-1), two peaks at 345nm and at 400nm were always observed during the study at all the pH levels before the kinetic studies. The peak at 345nm was almost stable during the time period, but the peak at 400nm increased by almost a factor of two over time, so the kinetics of the hydrolysis of RIM was studied at 400nm (unstable peak). The increase in the absorption at 400nm is greater than that at 345nm in every trial (including Figure 3.1-2), suggesting that the hydrolysis product formation is detectable and can be easily studied at 400nm. The absorptivity coefficient for RIM complex at 400nm is 831.2 $M^{-1}cm^{-1}$.

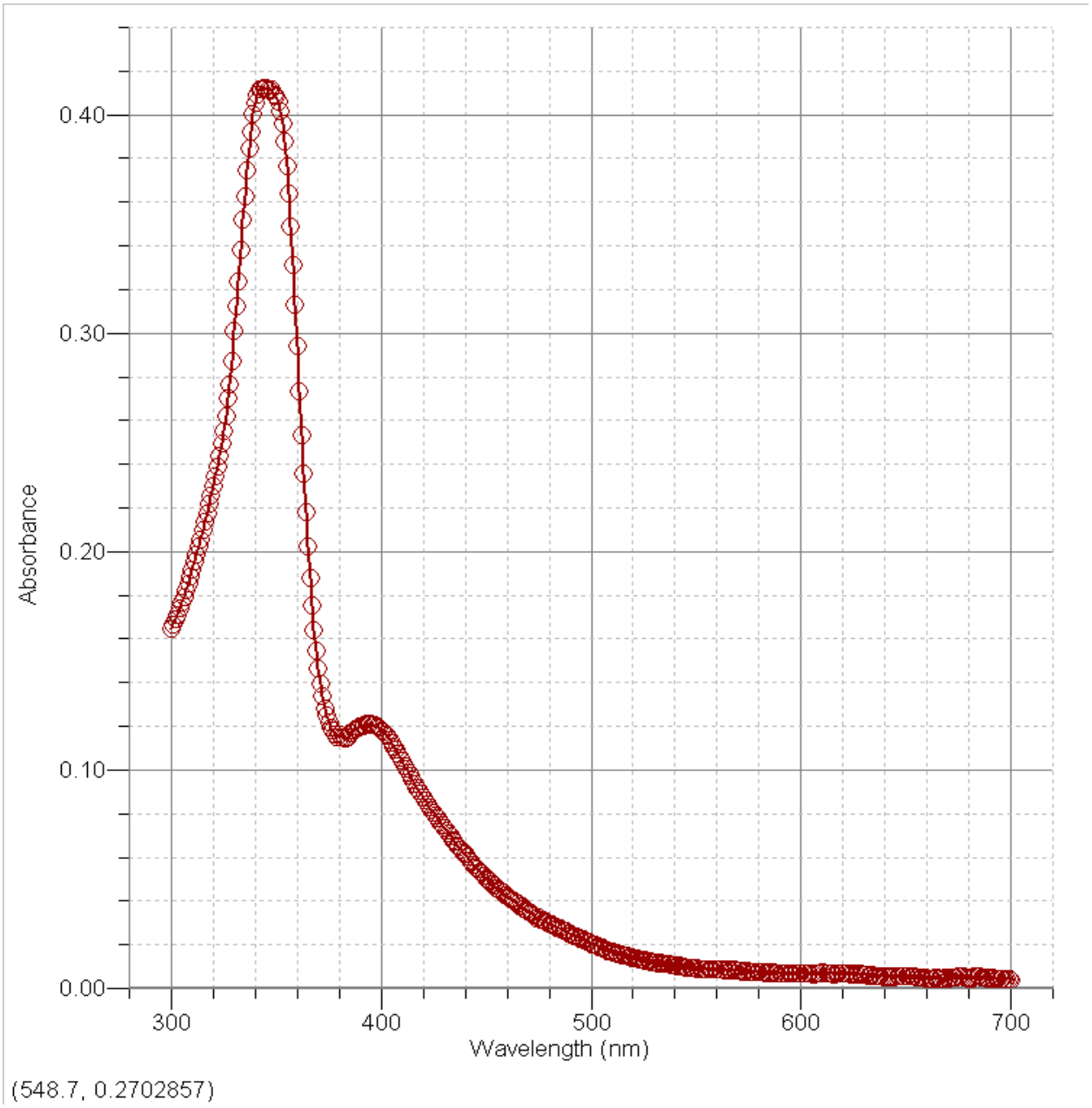

Figure 3.1-1 Absorbance spectrum of RIM at pH 4.2 (two peaks at 345nm and 400nm).

Figure 3.1-1 represents the normal absorption spectrum of RIM complex in any buffer at room temperature. The spectrum has two peaks, one at 345nm and the next at 400nm.

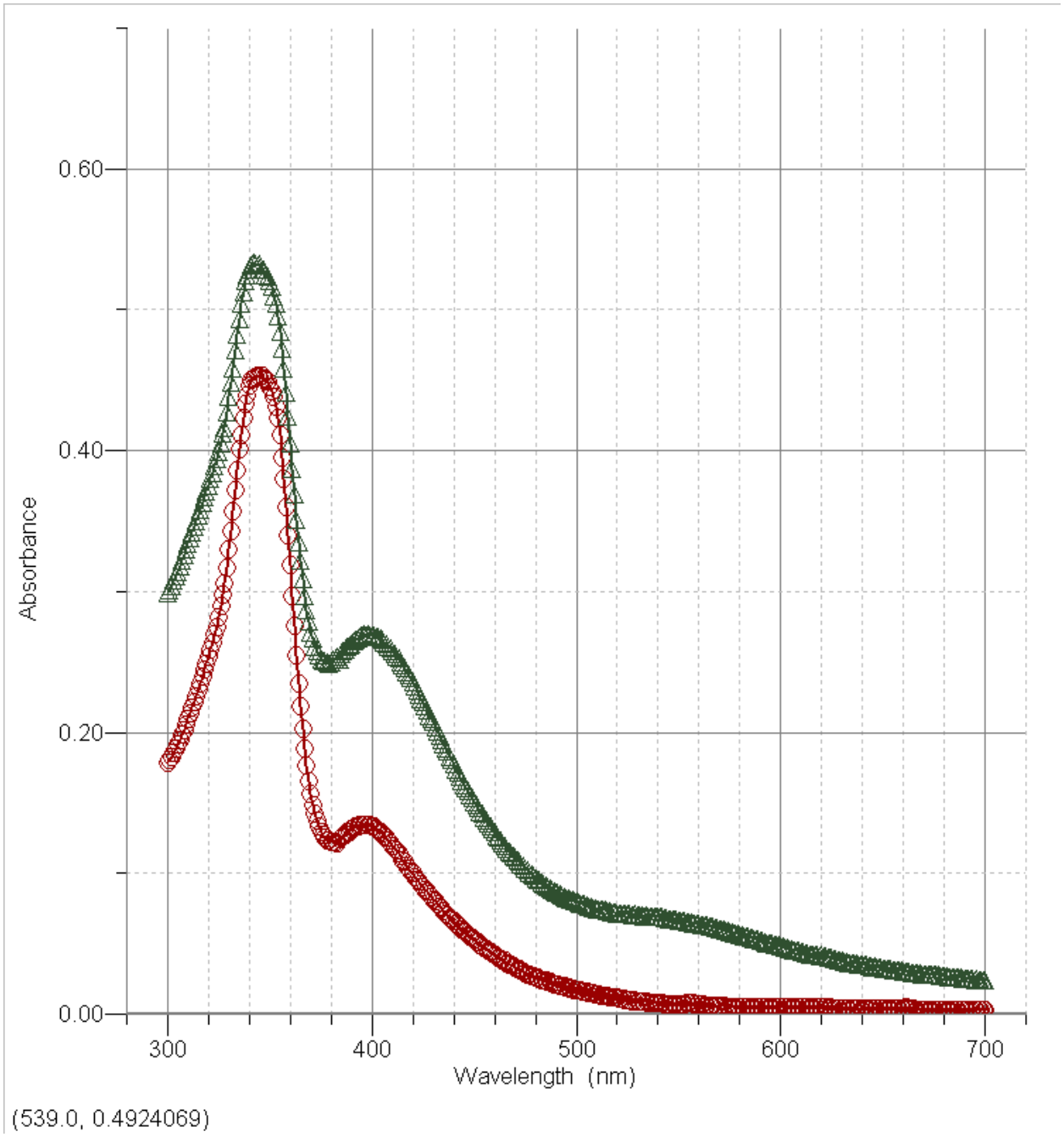

Figure 3.1-2 Absorbance spectrum of RIM at pH 6.4 over time (red curve with circles at 0 hrs and green curve with triangles at 5hrs).

The increase in the absorbance over 5 hrs at 345nm and 400nm can be observed in Figure 3.1-2, which is a hydrolysis graph of RIM complex at pH 6.4.

Figure 3.1-2 is the representative absorbance spectrum of the RIM complex before and after hydrolysis.

The following Figures (3.1-3 to 3.1-7) represent the hydrolysis of Ruthenium-imidazole (RIM), the first complex at room temperature at different pH (4.2, 6.4, 7.4, 8.4, and 9.4) levels for 6 hrs and 12 hrs (except at pH 4.2 for 24 hrs instead of 12 hrs).

Figures 3.1-3 and 3.1-4 represent the hydrolysis of Ruthenium-imidazole (RIM), the first complex at room temperature in acidic pH levels of 4.2 and 6.4. An induction period, which is hypothesized to be due to the formation of an intermediate in the reaction, was observed in all the acidic pH kinetic runs for the first 1 hr and then the hydrolysis products were seen to dominate the kinetics until 12 hrs and up to 24 hrs in few samples.

The first step of the reaction was very fast in all the hydrolysis reactions of RIM when compared with that of the second step of the reaction. As the pH increased, the rate of the first step of the reaction increased. So the basic pH promoted the formation of intermediate in the hydrolysis of the RIM complex.

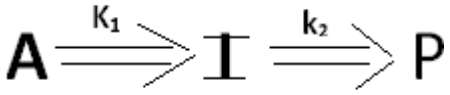

The hydrolysis reaction of the ruthenium imidazole complex can be represented as above in a two step process where A is the reactant, I is the intermediate, and P is the product, and k_1 and k_2 are the rate constants for the first and second steps respectively.

$$[A] = [A]_0 * e^{-k1t} \quad 2.3\text{-}1$$

$$[I] = (k_1 [A]_0/(k_2 - k_1))* (e^{-k1t} - e^{-k2t}) \quad 2.3\text{-}2$$

$$[P]= [A]_0 - [A] - [I] = [A]_0 * \{ 1+ [(1/(k_1-k_2))*(k_2 e^{-k1t} - k_1 e^{-k2t})]\} \quad 2.3\text{-}3$$

Equations 2.3-1 to 2.3-3 relate the actual concentrations of reactant final [A] and initial $[A]_0$, intermediate [I] and product [P] to time. All three equations are used to determine equation 2.3-5, which is used for the calculation of rate constant (k_1) for the first step of the reaction.

The Rate constants, k_1 and k_2, for each reaction were calculated using absorbances instead of concentration by the following equations:

The spectrum obtained for the kinetic study was analyzed graphically using graphical analysis software, and the "best fit" curve was used to obtain the rate of the reaction using the following equations:

Assuming $k_1 >> k_2$ (first step is very fast), the rate constant for the second step can be calculated by using the relation; total absorption (Abs_T) is the sum of the absorptions of intermediate (Abs_I) and product (Abs_P), $Abs_T = Abs_P + Abs_I$

$$Y = A^* (1-e^{-C^*x}) + B^*(e^{-C^*x}) \qquad 2.3\text{-}4$$

where C is the rate constant (k_2), for the second step of the reaction, Y is the total absorbance at any time, x is the time, B is the absorbance of intermediate, and A is the absorbance of the product. For this purpose the portion of the curve from 100 minutes (exponential part of the curve) is used instead of the full curve because there was an induction period observed within 100 minutes in all of the graphs. The second step rate constant (k_2) was calculated using equation 2.3-4.[42]

The rate constant for the first step (k_1) can be calculated by using the relation that total absorption (Abs_T) is the sum of the absorptions of reactant (Abs_R), intermediate (Abs_I), product (Abs_P), $Abs_T = Abs_R + Abs_I + Abs_P$

$$Y = A^*e^{-B^*x} + C^*\left(\frac{B}{D-B}\right)^*(e^{-B^*x}-e^{-D^*x}) + E^*\left(1+\left(\frac{1}{B-D}\right)^*(D^*e^{-B^*x}-B^*e^{-D^*x})\right) \qquad 2.3\text{-}5$$

Where A, C, and E are constants related to the absorbance of the reactant, intermediate, and product respectively, at longer times the intermediate concentration decays to zero,

B is the rate constant for the first step of the reaction (k_1), and

D is the rate constant for the second step of the reaction (k_2).

The rate constants for the first step of the reaction, which is the faster step, and the second step were obtained by fitting the curve graphically using graphical analysis software to equation 2.3-5 and using the best fit parameters.[43]

Both the equations 2.3-4 and 2.3-5 gave approximately similar values for the k_2 for all the hydrolysis reactions of RIM in different buffer solutions because the intermediate forms quickly within 100 minutes, and after 100 minutes we looked at the kinetics of only the second step.

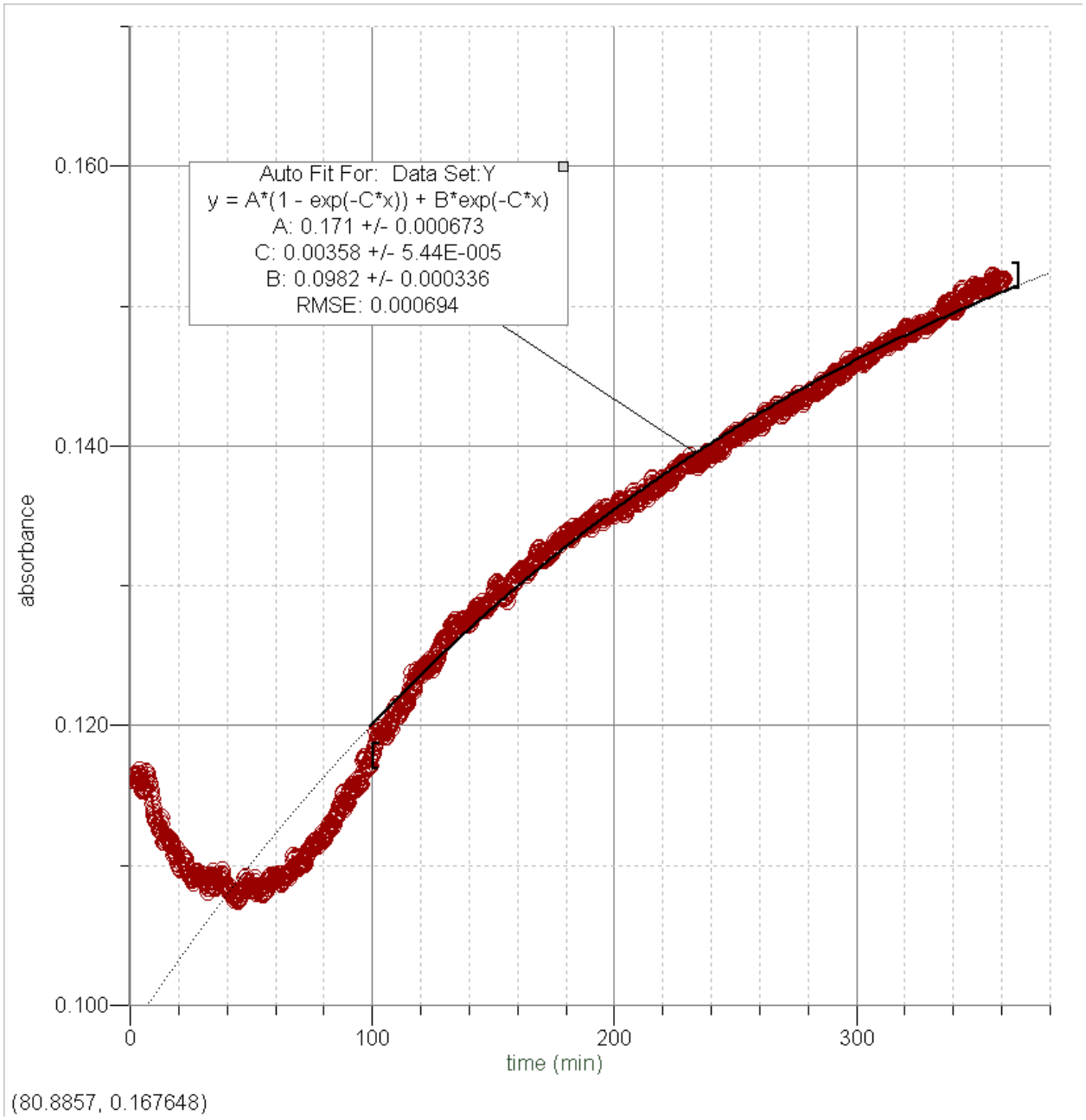

Figure 3.1-3 Hydrolysis of RIM at pH 4.2 for 6 hrs.

Figure 3.1-3 shows the hydrolysis of RIM at pH 4.2 for 6 hrs. For the first 100 minutes there was an induction period, and then the rate of hydrolysis increased. The hydrolysis was observed to be of first order with a rate constant (k_2) of 0.00358 per sec.

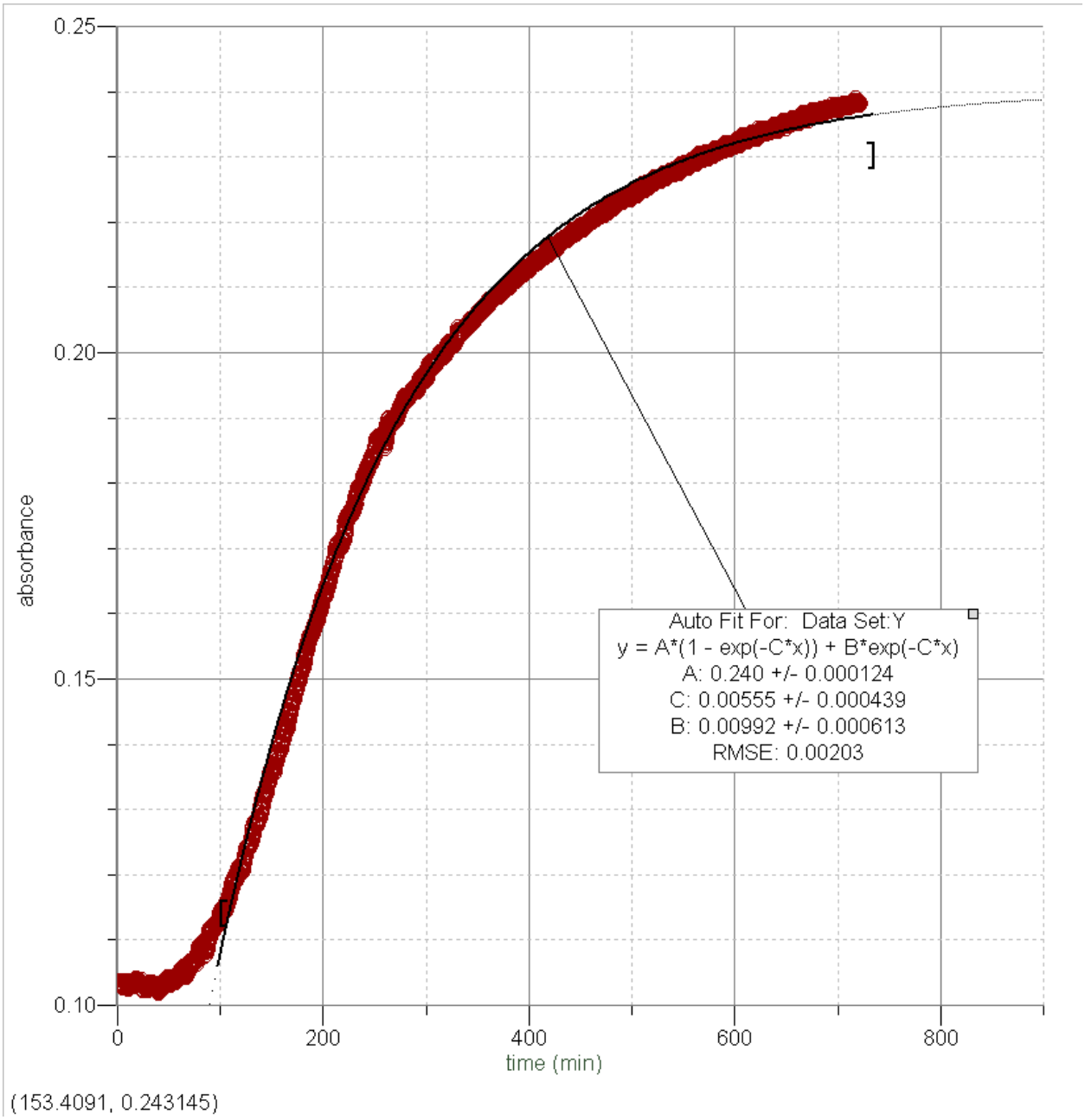

Figure 3.1-4 Hydrolysis of RIM at pH 6.4 for 12 hrs.

In the hydrolysis study of RIM at pH 6.4 for 6 hrs (Figure 3.1-4), for the first 1 hr there was an induction period, and then the rate of hydrolysis increased. The hydrolysis was observed to be of first order with a rate constant (k_2) of 0.00555 per sec.

Figures 3.1-5 to 3.1-7 represent the hydrolysis of Ruthenium-imidazole (RIM), the first complex at room temperature in basic pH levels of 7.4, 8.4, and 9.4. An induction

period, which is hypothesized to be due to the formation of an intermediate in the reaction, was briefly observed in the pH 7.4 kinetic runs, but there was no induction period observed in the graphs of pH 8.4 and 9.4 in the first hour; instead, hydrolysis started in the first 10 minutes. This might be because the intermediate formation is very fast at higher pH levels. The rate constants were fit with the model discussed for the acidic pH experiment above.

The induction period was significantly shorter in the graphs (Figures 3.1-6 to 3.1-8) of hydrolysis of RIM in pH solutions 8.4 and 9.4. The absorbance was stable initially for 20 minutes, and then there was an increase in the absorbance after 20 minutes. These results tell us that the formation of intermediate and the product is very fast at higher pH.

The hydrolysis reaction of the RIM complex was found to be a two-step process, and both the steps followed first order kinetics. Rate constants (k_1 and k_2) for the two steps were derived for the hydrolysis of RIM in all the buffer solutions (pH 4.2 to 9.4).

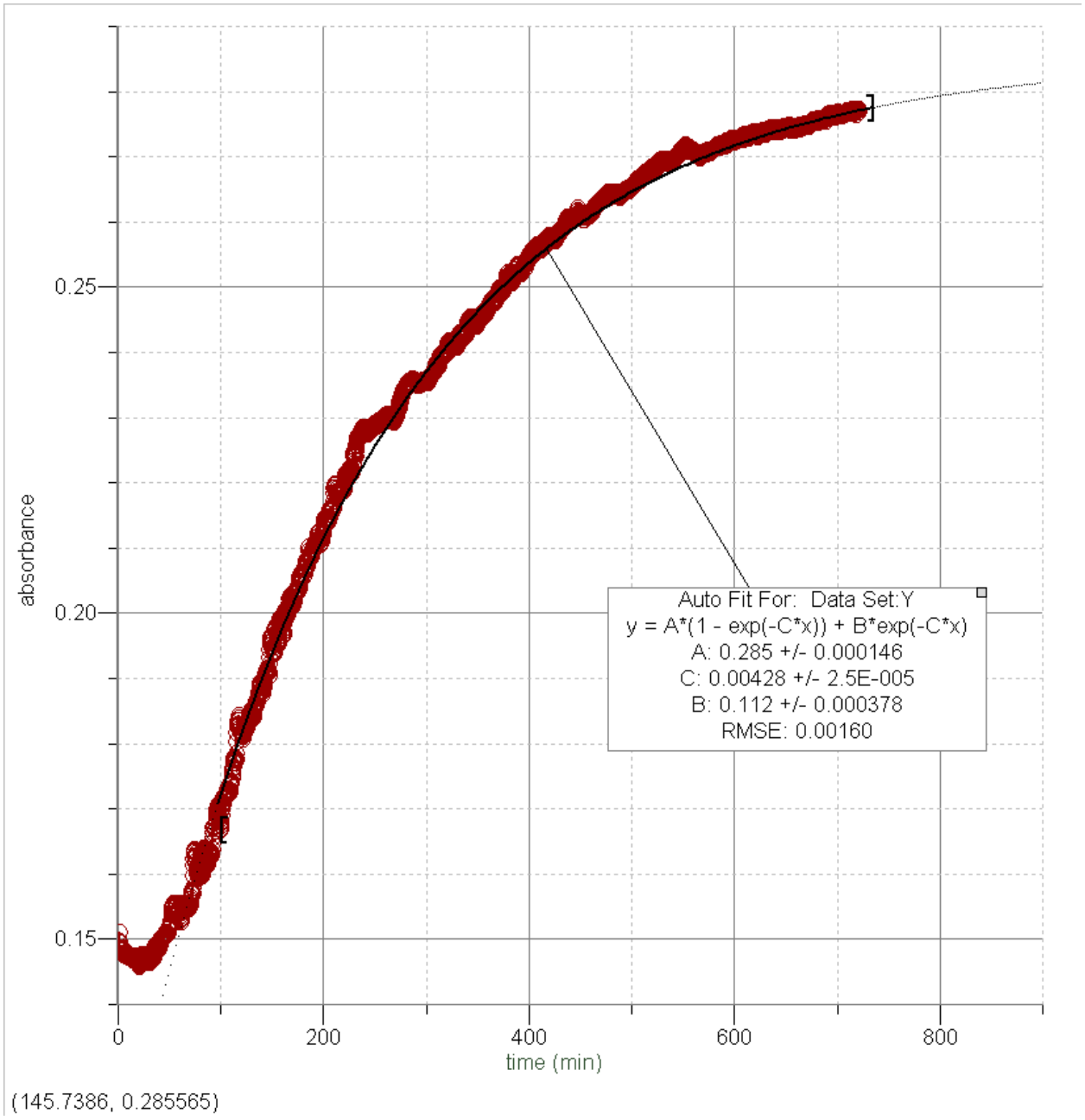

Figure 3.1-5 Hydrolysis of RIM at pH 7.4 for 12 hrs.

Figure 3.1-5 represents the hydrolysis of RIM at pH 7.4 for 12 hrs; for the first 1/2 hr there was an induction period, and then the rate of hydrolysis increased. The hydrolysis was observed to be of first order with a rate constant (k_2) of 0.00428 per sec.

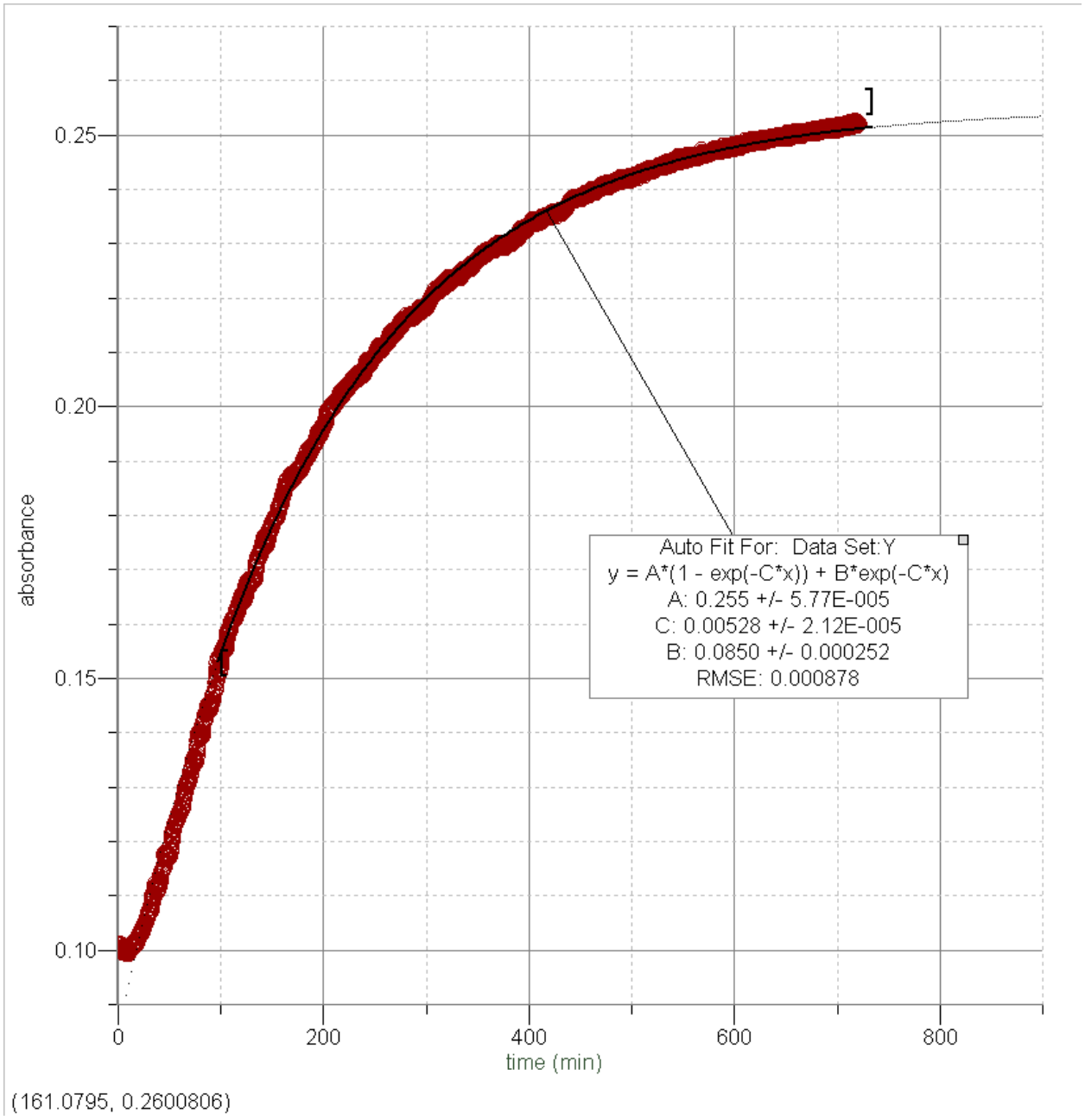

Figure 3.1-6 Hydrolysis of RIM at pH 8.4 for 12 hrs.

Figure 3.1-6 represents the hydrolysis of RIM at pH 8.4 for 12 hrs; for the first 20 minutes there was an induction period, and then the rate of hydrolysis increased. The hydrolysis was observed to be of first order with a rate constant of (k_2) 0.00528 per sec.

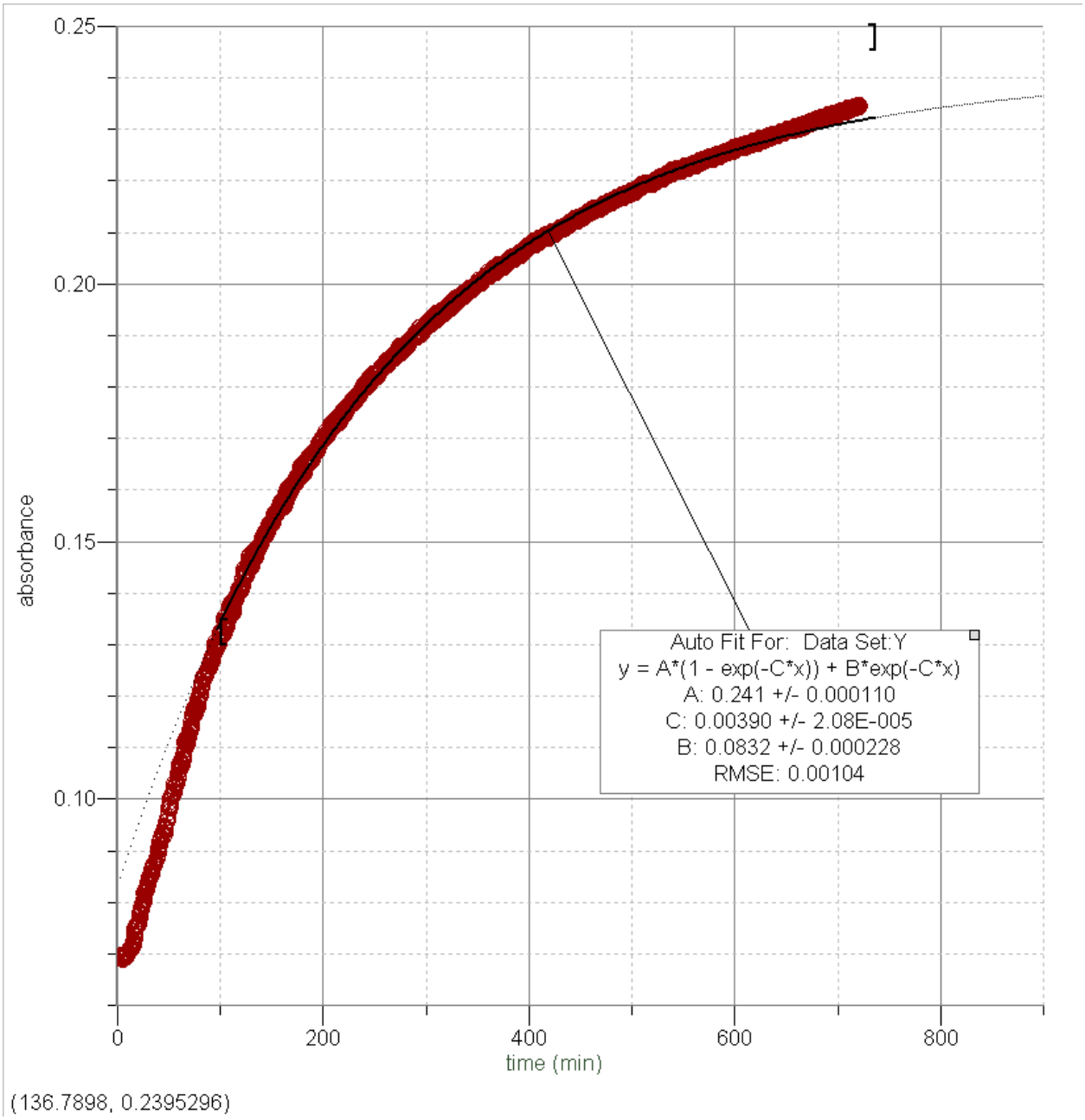

Figure 3.1-7 Hydrolysis of RIM at pH 9.4 for 12 hrs.

Figure 3.1-7 represents the hydrolysis of RIM at pH 9.4 for 12 hrs. There was not much initial induction period; instead, the hydrolysis was observed immediately after 10 minutes. The hydrolysis was observed to be of first order with a rate constants k_2= 0.00390 per sec.

Table 3.1-1 Average rate constants for two steps (k_1= first step and k_2= second step) of the hydrolysis of RIM complex at different pH.

pH	k_1 of all Runs (per sec)		Average k_1 (per sec)	k_2 of all Runs (per sec)		Average k_2 (per sec)
4.2	Run1	0.0334	0.0494	Run1	0.00358	0.00236
	Run2	0.0654		Run2	0.00115	
6.4	Run1	0.0275	0.0271	Run1	0.00555	0.00548
	Run2	0.0267		Run2	0.00541	
7.4	Run1	0.0178	0.0203	Run1	0.00596	0.00645
	Run2	0.0179		Run2	0.00428	
	Run3	0.0251		Run3	0.00913	
8.4	Run1	0.0298	0.0502	Run1	0.00873	0.00780
	Run2	0.0247		Run2	0.00528	
	Run3	0.0961		Run3	0.00940	
9.4	Run1	0.0418	0.0268	Run1	0.00574	0.00482
	Run2	0.0119		Run2	0.00390	

Table 3.1-1 represents the average rate constants for the two steps of the hydrolysis reaction of RIM complex at room temperature in different pH buffers. The reaction rate (k_1) for the first step did not follow a specific trend because the rate of hydrolysis decreased from pH 4.2 to 7.4 and then increased up to pH 8.4, after which the rate decreased for pH 9.4. However, the rate constant for the second step of the reaction (k_2) was found increasing as the H increased, except at pH 9.4 (decreased). The first step in the hydrolysis reaction of RIM complex is 10 times faster than the second step ($k_1 >> k_2$, from Table 3.1-1).

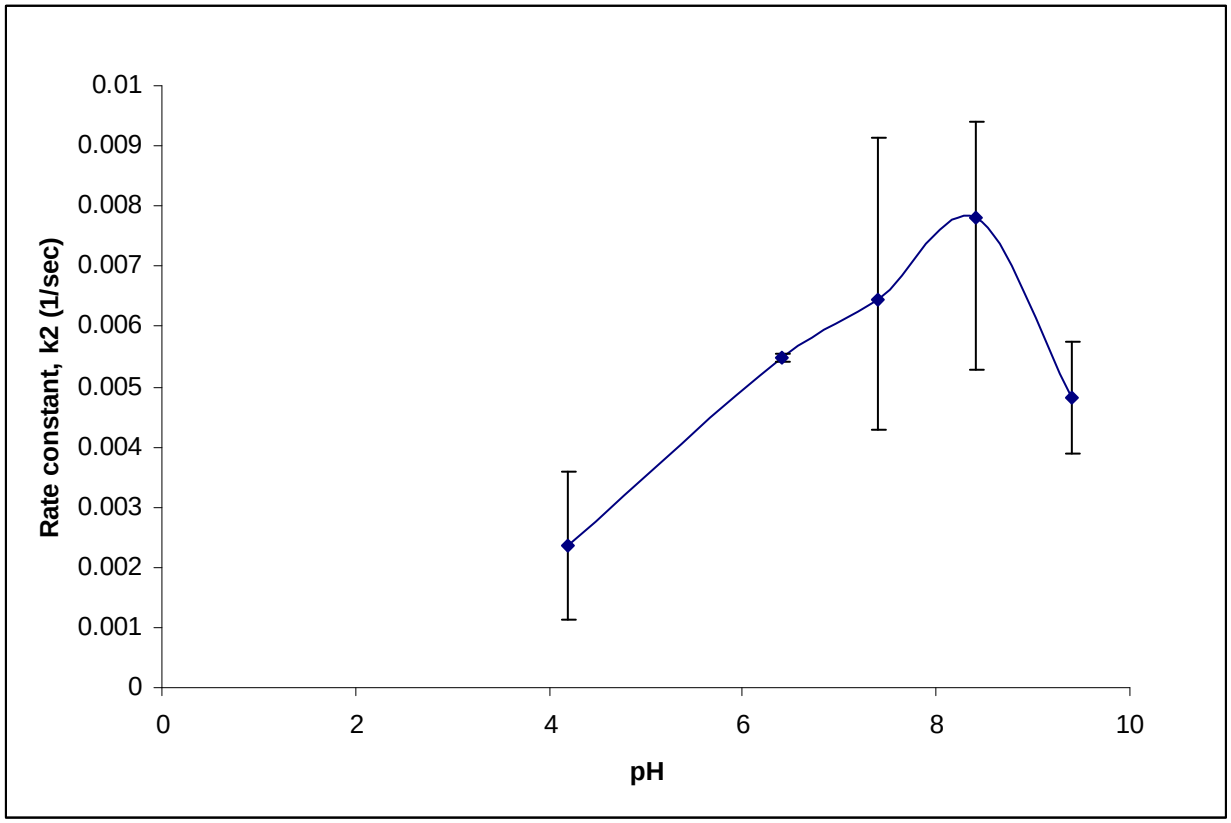

Figure 3.1-8 Hydrolysis profile of RIM complex (effect of pH on k_2).

Figure 3.1-8 represents the hydrolysis profile of second step in the hydrolysis of Ruthenium-Imidazole complex at different pH levels. The error bars were calculated by considering the values of all the runs and their deviation from the average (±0.00122, ±0.00007, 0.00217/0.00268, 0.00160/0.00252 and ±0.00092, for studies at pH 4.2, 6.4, 7.4, 8.4 and 9.4 respectively). As the basicity and acidity increased, the range of error decreased. The range of error was high at pH 7.4 and 8.4.

3.2 Ruthenium-Indazole Complex (RIN)

The normal absorbance spectrum of RIN has four peaks at 210nm, 241nm, 287nm, and 360nm, as seen in Figure 3.2-1. The peak at 287nm experienced greater variation in size over time, compared with other three peaks, so the kinetics of the hydrolysis reaction was studied at wavelength 287nm for RIN as illustrated in Figure 3.2.2. The absorptivity coefficient for the RIN complex at 287 nm is 8810 $M^{-1}cm^{-1}$.

Figures 3.2-2 to 3.2-4 show how the absorption spectrum of RIN complex changes over time at different pH values (5.4, 8.4, and 9.4 respectively).

Figure 3.2-4 shows that the absorption spectrum, between 0 and 10 minutes, changes from four peaks to two peaks, which may imply that the hydrolysis of RIN is a complex process.

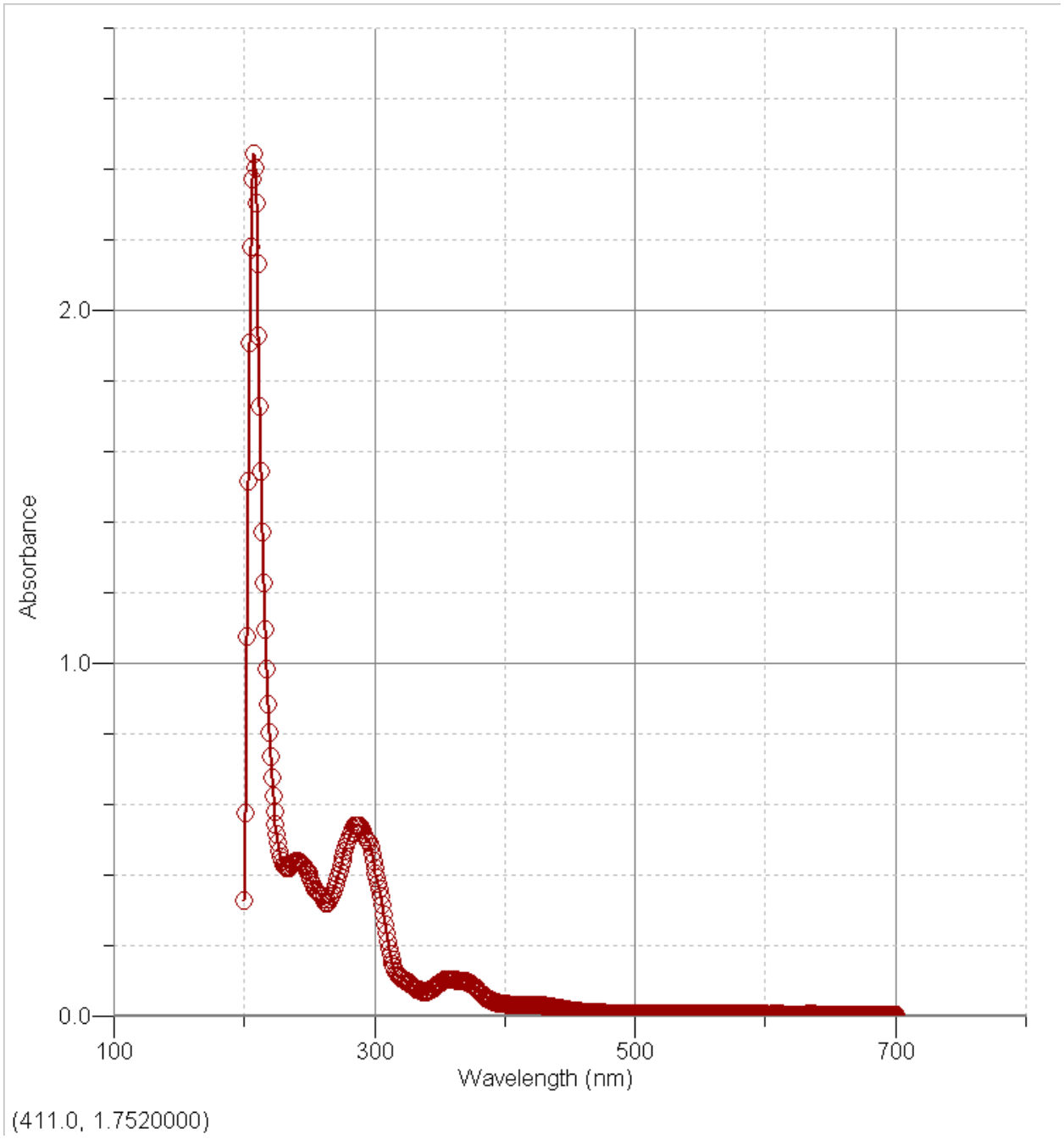

Figure 3.2-1 Absorbance spectrum of RIN at pH 7.4 (four peaks at 210nm, 241nm, 287nm and 360nm).

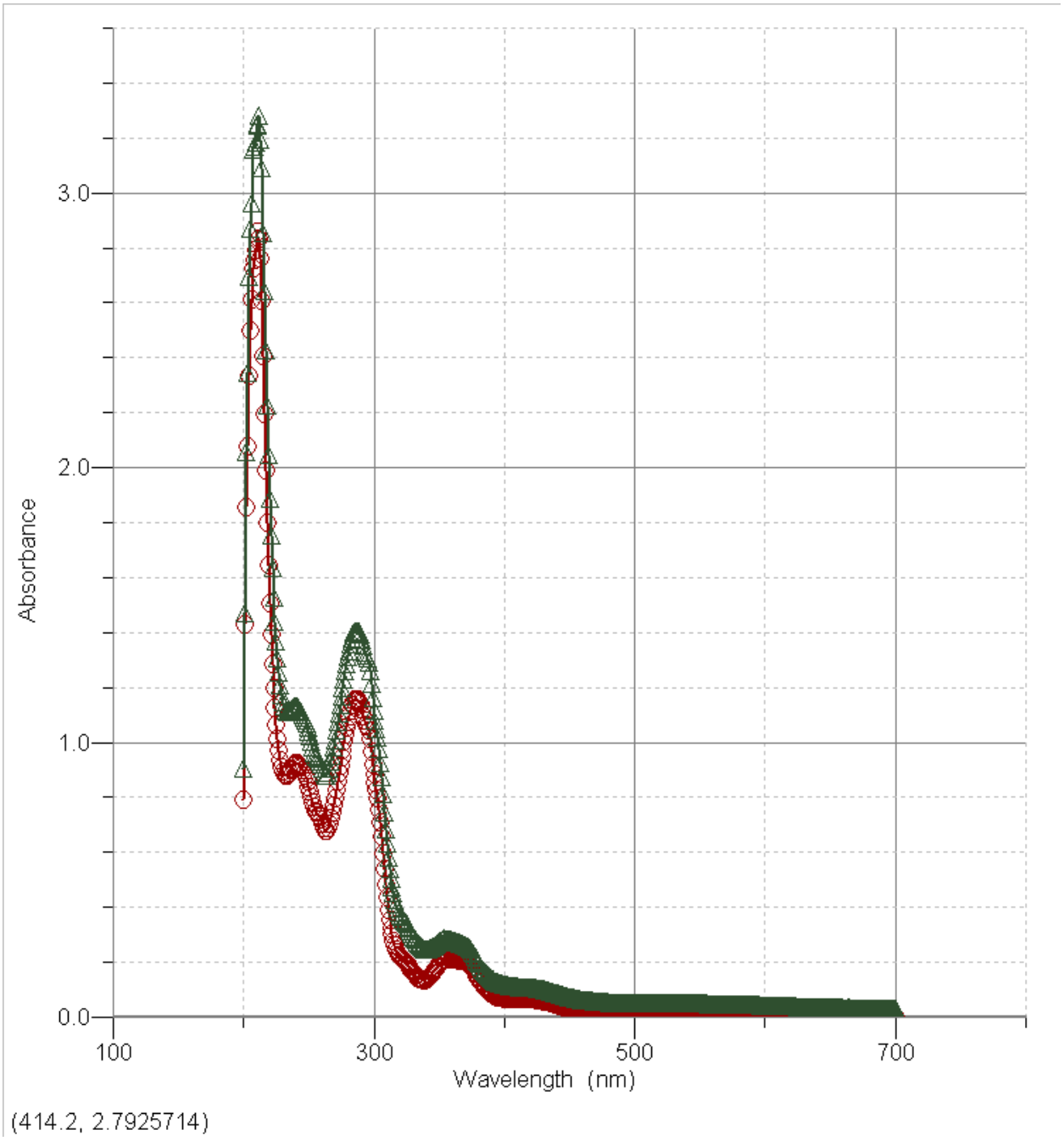

Figure 3.2-2 Absorbance spectrum of RIN at pH 5.4 over time (red curve with circles at 0 hrs and green curve with triangles at 6 hrs).

From Figure 3.2-2, the increase in the absorbencies at all four peaks is clear for the RIM complex hydrolysis at pH 5.4.

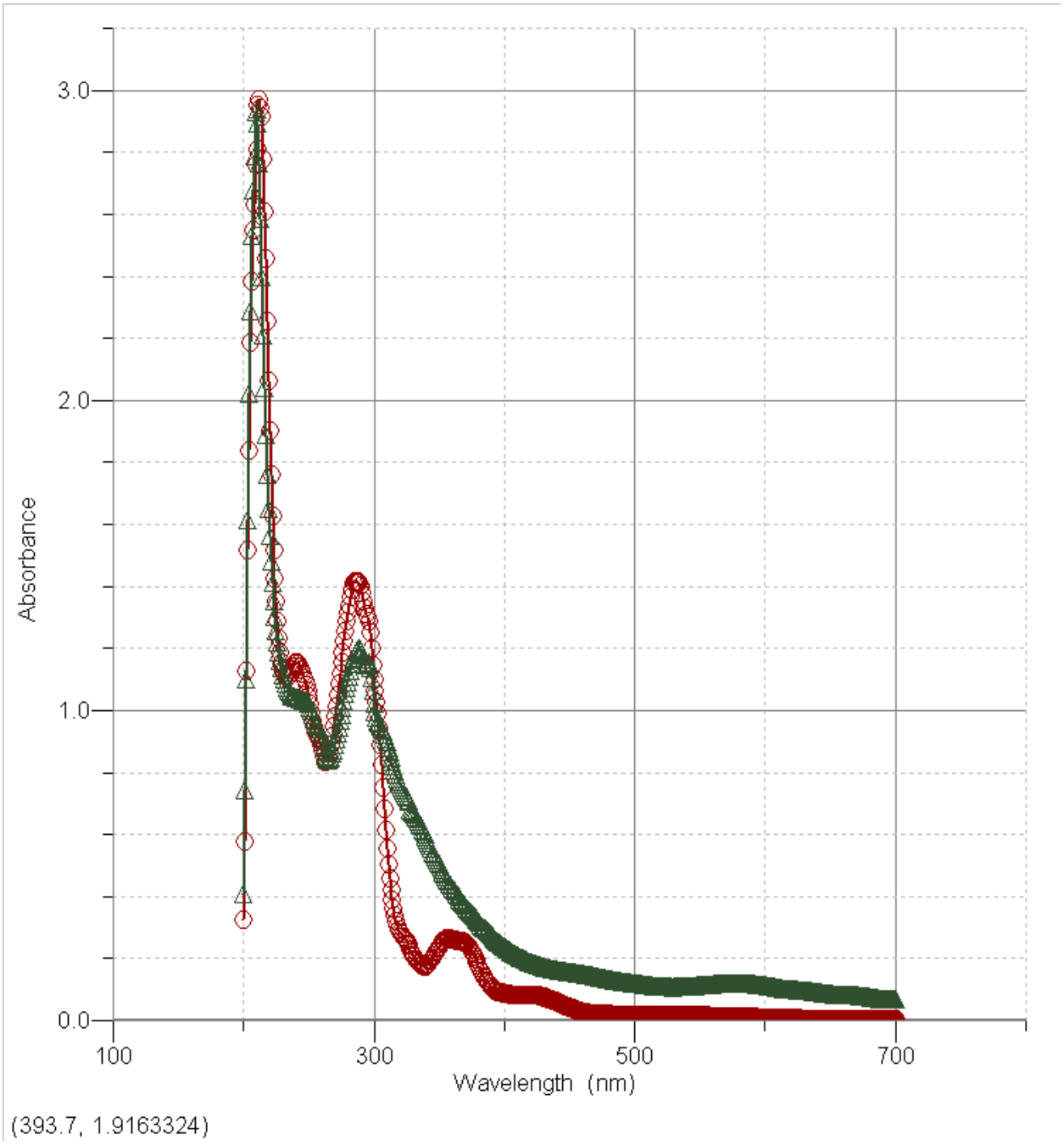

Figure 3.2-3 Absorbance spectrum of RIN at pH 8.4 over time (red cure with circles at 0 hrs and green curve with triangles at 1 hr).

From Figure 3.2-3, the decrease in the absorbencies at the three peaks (210nm, 241nm and 287 nm), the near elimination of the second peak at 241nm, and the elimination of 4th peak at 360nm are clear for the RIN complex hydrolysis at pH 8.4.

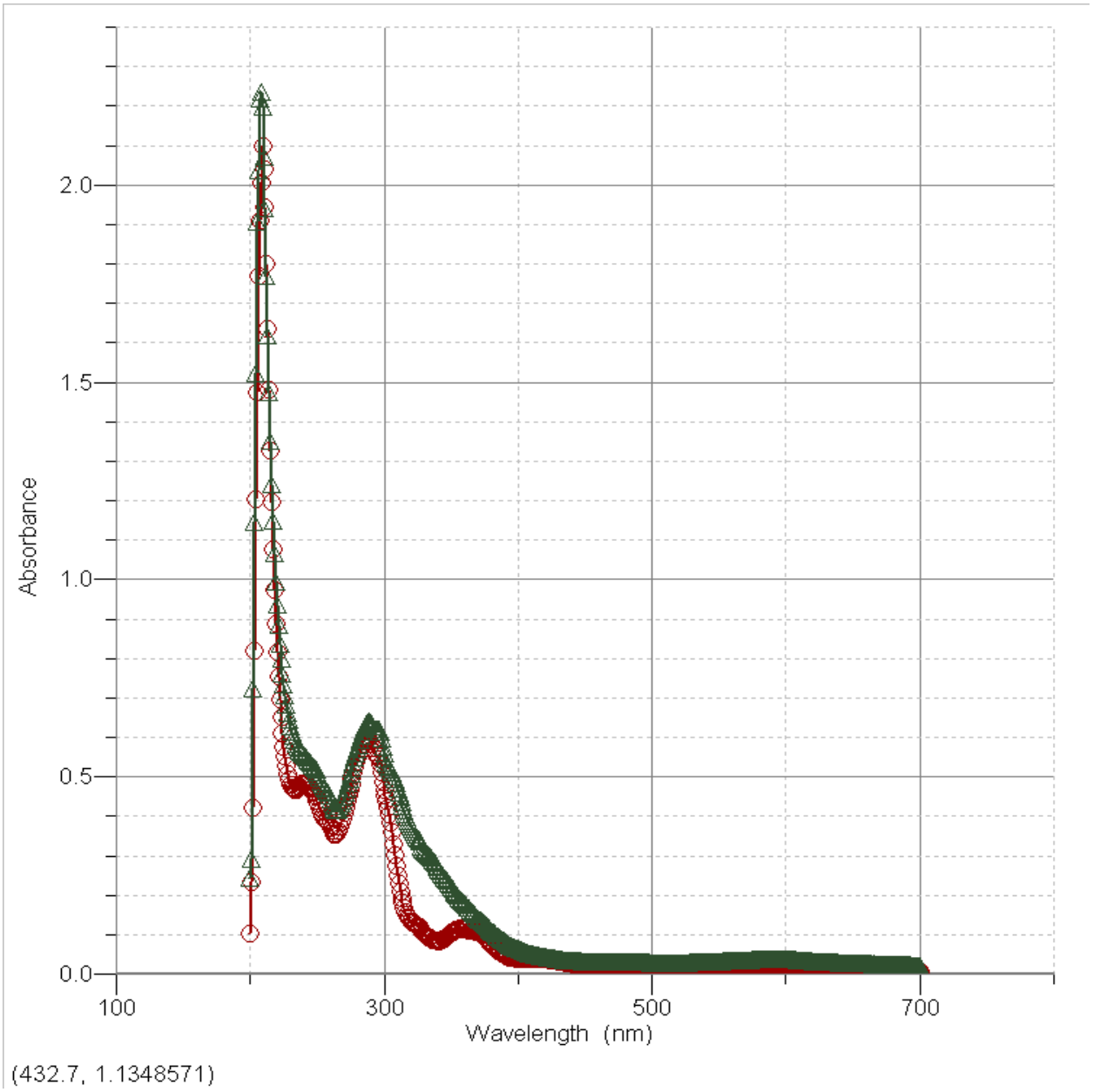

Figure 3.2-4 Absorbance spectrum of RIN at pH 9.4 over time (red curve with circles at 0 hrs and green curve with triangles at 10 minutes).

Figures 3.2-5 to 3.2-10 show the time variation of the absorbance at 287nm due to the hydrolysis of RIN complex at pH 4.2, 5.4, 6.4, 7.4, 8.4 and 9.4 respectively.

From these figures we observed that the hydrolysis was fast for the RIN complex. The complete hydrolysis reaction was observed to occur within the first 1 hr for solutions of

pH 4.2 to 6.4, and then the absorbance was stable after that. But from pH 7.4 to 9.4 the hydrolysis was very fast and observed within the first 15 minutes, faster than the hydrolysis observed in solutions of pH 4.2 to 6.4. But at higher pH (7.4 to 9.4), the peaks at 241nm and 360nm started disappearing as shown in Figures 3.2-3 and 3.2-4. There were only two peaks visible after 15 minutes of the study in the RIN solution at pH 9.4 (Figure 3.2-4).

The signature of the curve was not retained at higher pH levels, which indicates a more complex reaction mechanism of the hydrolysis of RIN complex, which may be due to formation of intermediates or the formation of products in different possible steps of the mechanism (as shown in Figure 1.5-1).

The indazole (pK_a 1.25) is less basic than imidazole (pK_a 7.11), which suggests that indazole is a less potent sigma bond donor than imidazole. As the basicity of imidazole is high, the energy of the excited state is also high. As a result, the less stable RIN complex reacts faster at higher pH. This was also observed and stated in earlier studies.[8]

The higher basicity affects the absorbance of this species more than the RIM and thus makes quantitative analysis of the data very difficult to perform, but qualitatively it can be seen that the kinetics is faster for RIN than RIM.

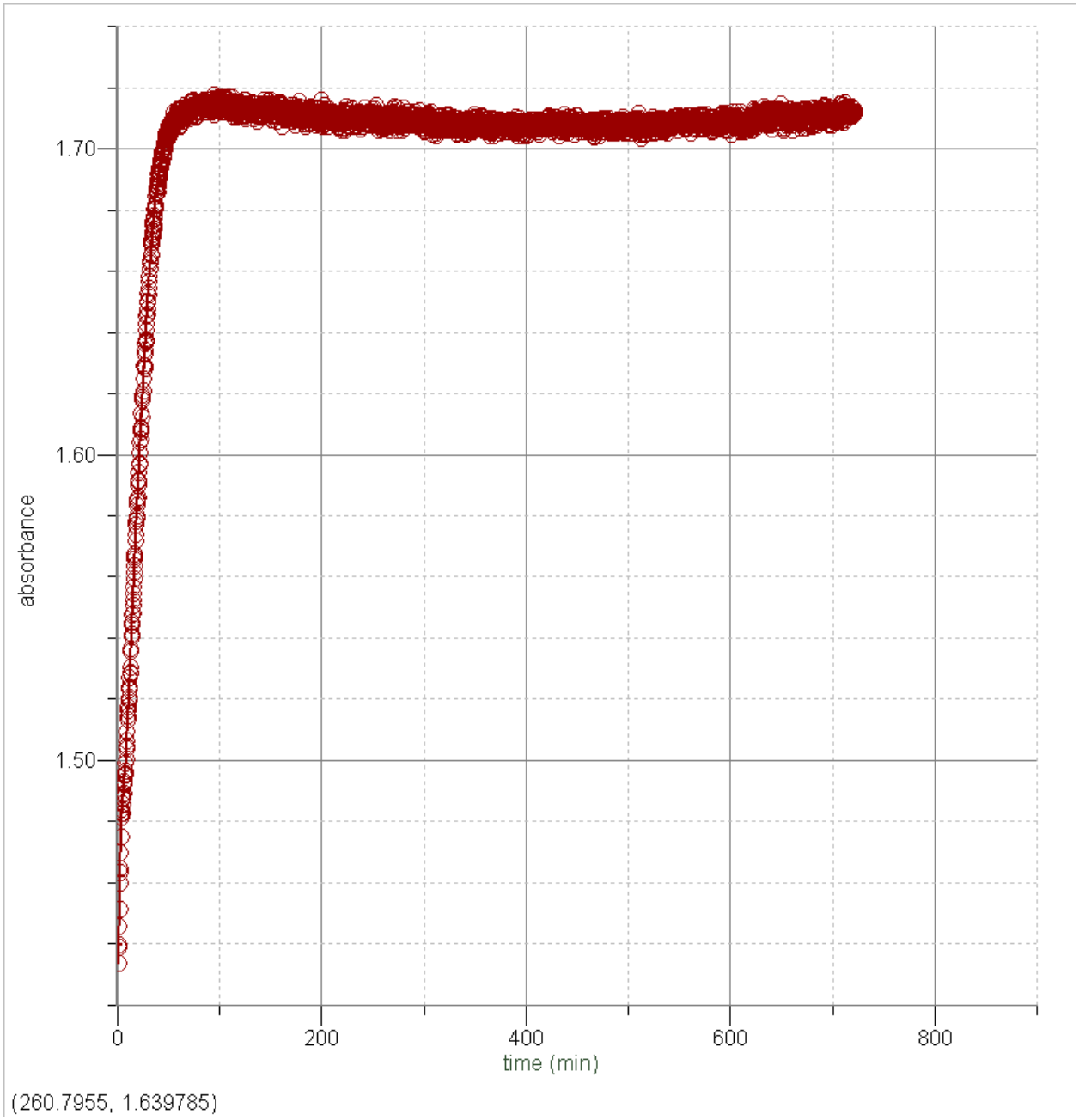

Figure 3.2-5 Hydrolysis of RIN at pH 4.2 for 12 hrs.

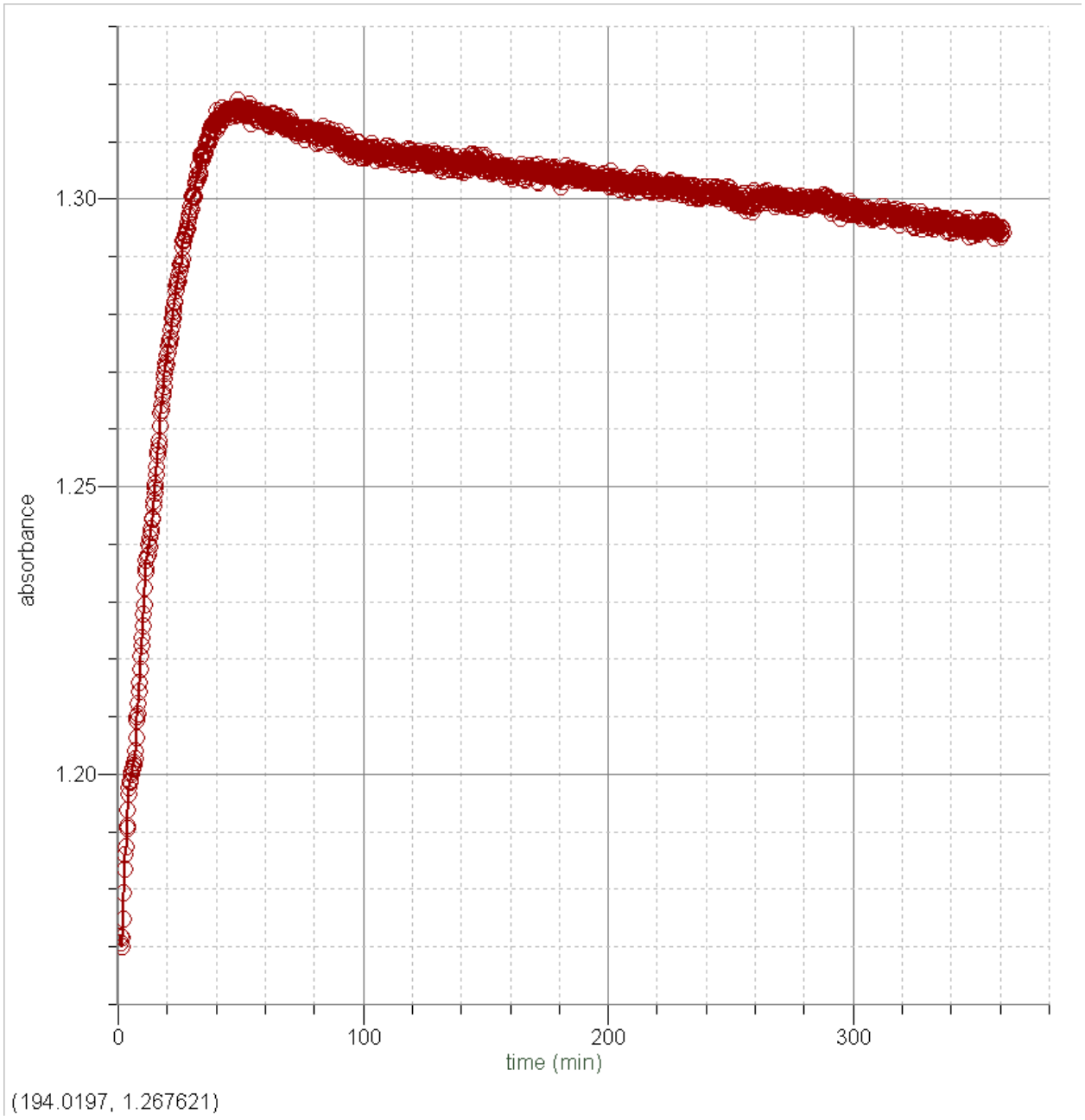

Figure 3.2-6 Hydrolysis of RIN at pH 5.4 for 6 hrs.

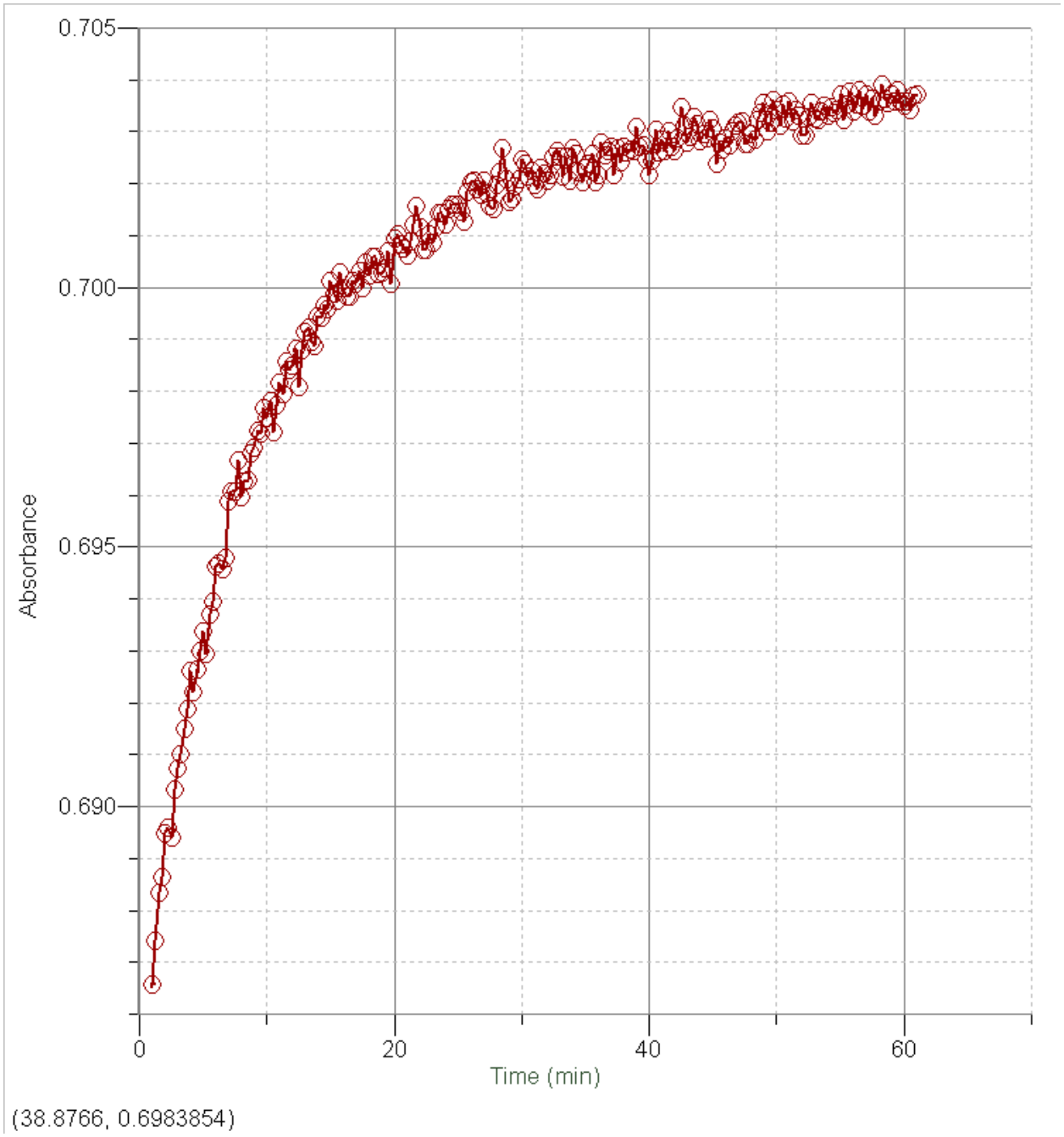

Figure 3.2-7 Hydrolysis of RIN at pH 6.4 for 1 hr.

Figures 3.2-8 to 3.2-10 show the hydrolysis reaction monitored at 287 nm for neutral and basic pH. Contrasted to the acidic pH, the curve at basic pH decreases with time. This seems to indicate that the signature of the absorbance spectrum changes with pH for this complex hydrolysis product.

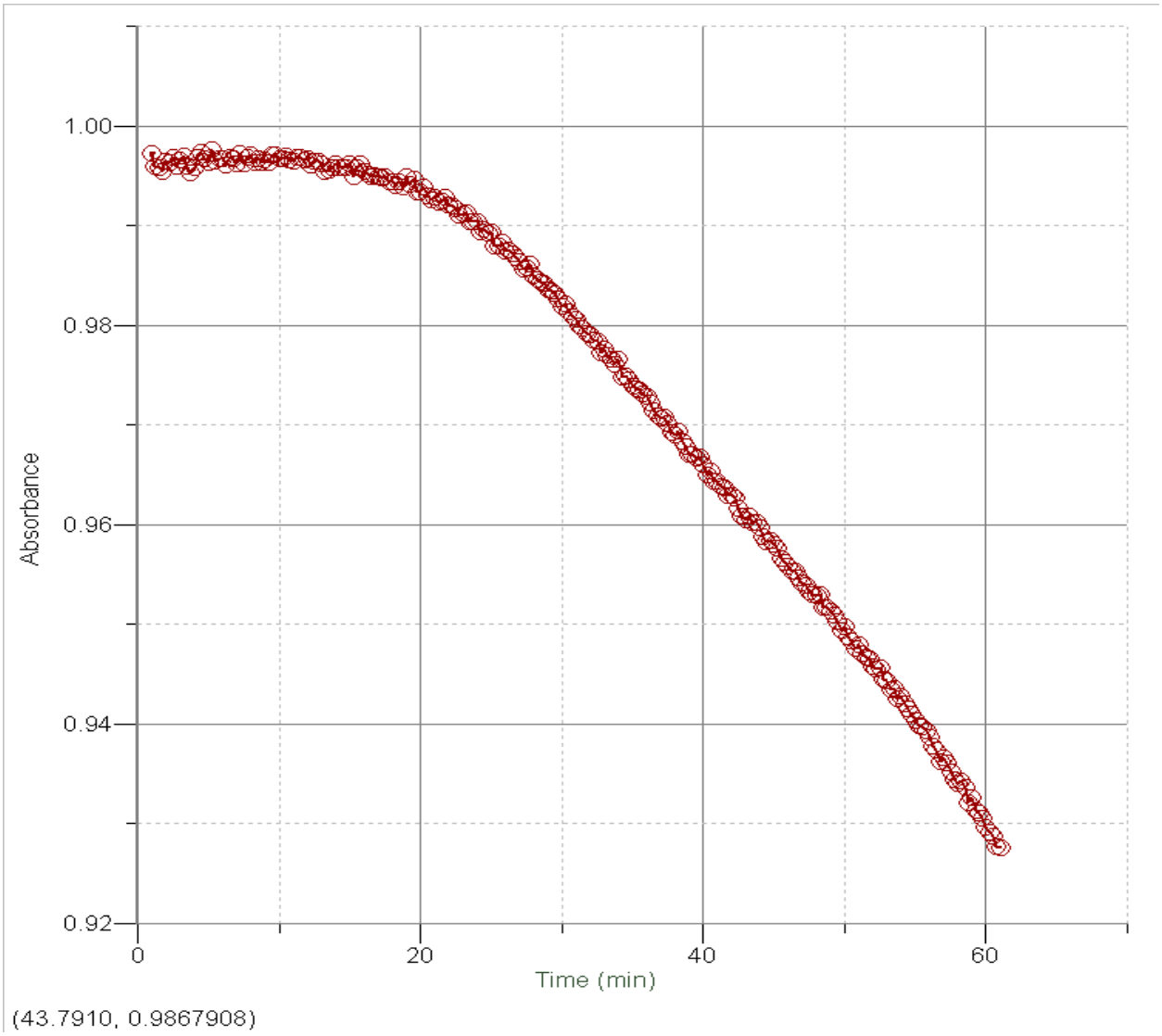

Figure 3.2-8 Hydrolysis of RIN at pH 7.4 for 1 hr.

The hydrolysis was fast, hence the curve was stable for the first 10 minutes and then the decay in the curve for RIN complex at pH 7.4 occurred (Figure 3.2-8), indicating early formation of hydrolysis product.

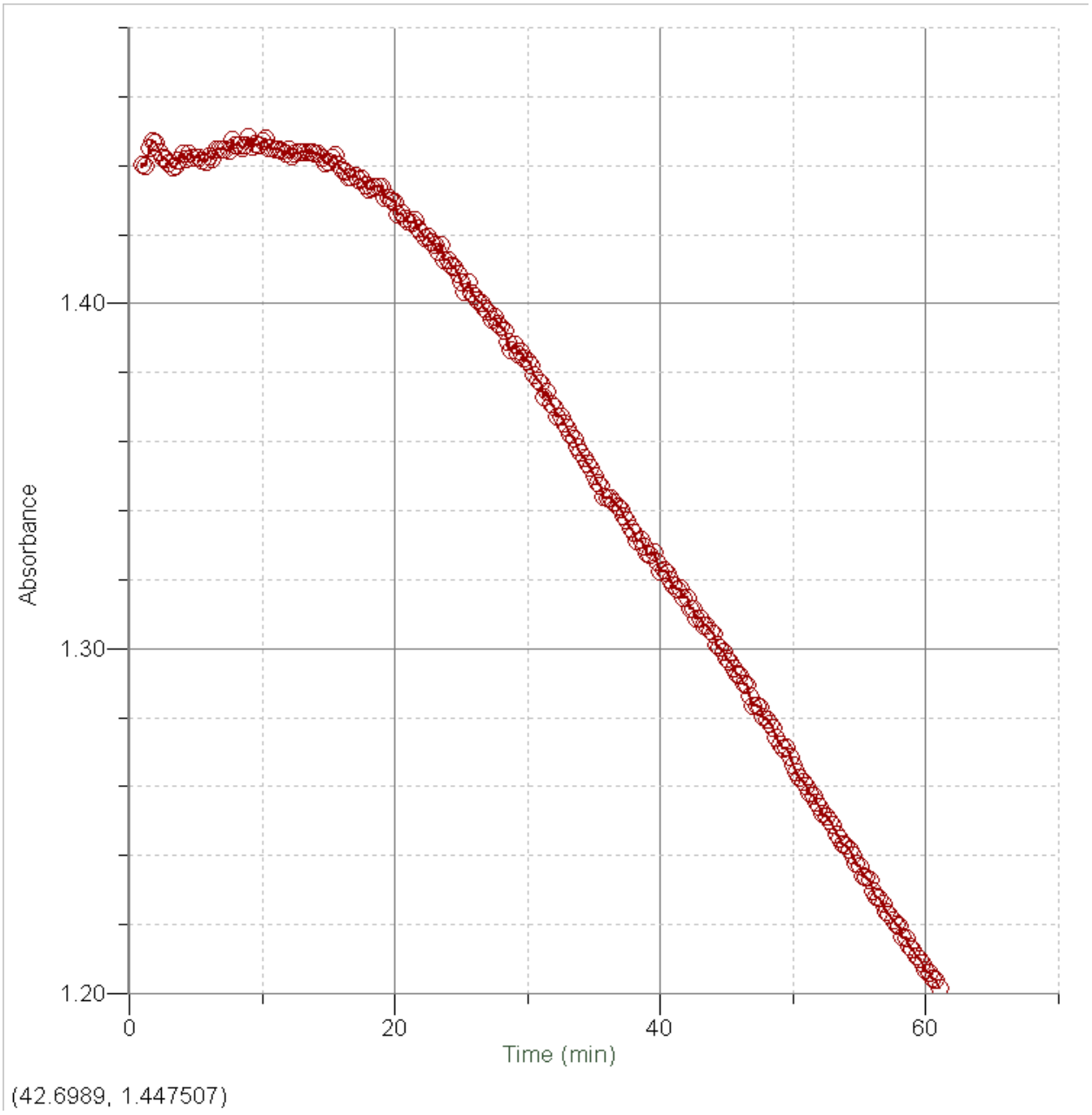

Figure 3.2-9 Hydrolysis of RIN at pH 8.4 for 1 hr.

The hydrolysis was very fast, hence we observed a stable curve for the first 10 minutes and then decay was seen for RIN complex at pH 8.4 (Figure 3.2-9), indicating early formation of hydrolysis product.

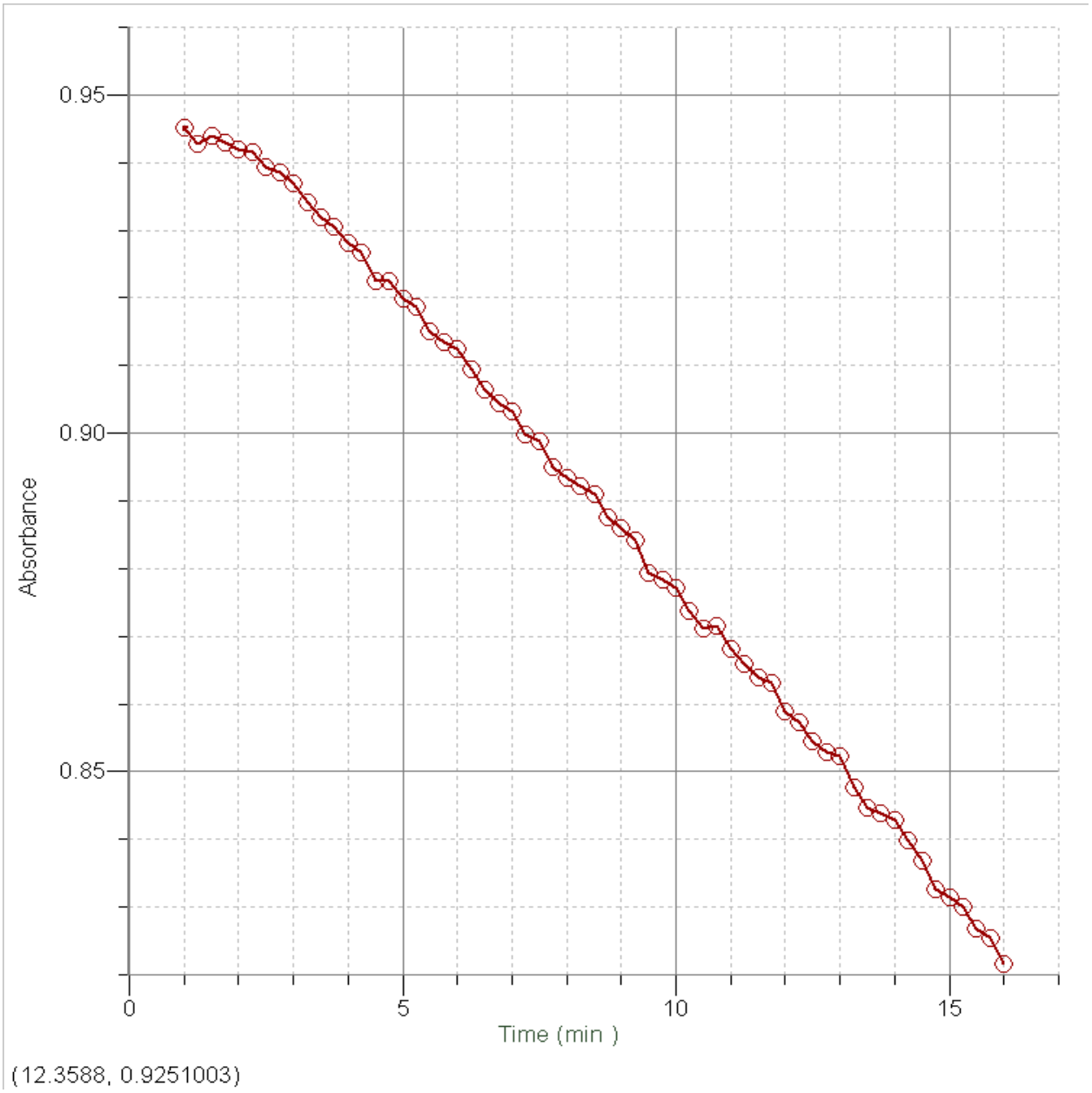

Figure 3.2-10 Hydrolysis of RIN at pH 9.4 for 15 min.

The hydrolysis process is very fast as the curve was decaying immediately within 15 minutes for RIN complex at pH 9.4 (Figure 3.2-10), indicating earlier formation of hydrolysis product. Further studies must be done to truly understand the number of intermediates, products, kinetic processes, and rate constants for the RIN hydrolysis.

CHAPTER 4: Conclusions

The hydrolysis process required more time to occur for RIM complexes than RIN complexes. The graphs of hydrolysis of RIM in pH solutions 4.2-7.4 show an induction peak within the first 100 minutes of the reaction, and then the hydrolysis was observed to continue for at least 12 hrs in all the solutions and up to 24 hrs in some of the solutions (at pH 4.2 and 6.4). It means that there is a formation of an intermediate before the formation of the hydrolysis product in this reaction.

There was no induction period observed in the hydrolysis reaction of the RIN complex (Figures 3.2-5 to 3.2-10). There was an immediate rise in absorbance at the beginning of the hydrolysis curve. The rise in absorbance was observed for the first hr at acidic pH and for a few minutes at neutral pH, and then no rise in absorbance was observed at basic pH; instead, the curve was decaying within the first 15 minutes of the study.

The normal absorbance spectrum of RIN complex always showed four peaks at 210nm, 241nm, 287nm, and 360nm in the solutions at different pH (e.g., see Figure 3.2-1). In the RIN complex solutions of pH 4.2 to 6.4, the absorbance of all the peaks was increased over time, especially at peak 287 nm, and was detectable (e.g., see Figure 3.2-2).

The basic pH might have promoted the faster hydrolysis of RIN complex. Hence the rise in the curve (formation of hydrolysis product) was not observed above pH 8.4 and was not detected, even in the first 15 minutes of the study.

The hydrolysis reaction is much faster for the RIN complex than the RIM complex. The hydrolysis of the RIN complex is dependent on pH, but the hydrolysis of the RIM complex is independent of pH (at higher pH levels). The rate of hydrolysis seems to increase for the RIN complex with an increase in pH or basicity. The hydrolysis reaction mechanism for the RIN complex was more complex than the RIM complex.

The effect of ligand on the hydrolysis of ruthenium complex was studied and found that rate of hydrolysis increased with indazole as ligand more than that of imidazole as ligand. The indazole (pK_a 1.25) is less basic than imidazole (pK_a 7.11), suggesting that indazole is a less potent sigma bond donor than imidazole. The higher the basicity, the higher the energy of the excited state. As a result, the less stable RIN complex reacts faster at higher pH.[8] The rate of active drug formation is high for RIM complex in the blood (rate constant, k_2 at pH 7.4, from table 3.1-1 and Figure 3.1-8) and hence it can be a good choice for controlling the rapidly growing cancer cells in initial stages of the disease.

Future studies

The hydrolysis products of the RIN complex at different intervals of time, if studied with HPLC and NMR spectroscopy, may reveal the actual structures of the intermediates or products formed. It also helps in understanding the steps or different pathways involved in the hydrolysis of the RIN complex. The hydrolysis studies at different temperatures and in different solvents with different pH may reveal more information about the hydrolysis kinetics of ruthenium complexes. The study of additional ligands like pyridine, thiazole, phenanthrolines, and their derivatives, and so on, will allow us to further understand the effect of basicity on the rate of hydrolysis of ruthenium complexes, because the donor properties of these molecules are similar to that of the purine and pyrimidine bases of DNA, which is the site of action for any cancer drug.

References:

1. Piccioli, F.; Sabatani, S.; Messori, L.; Orioli, P.; Hartinger, C. G.; Keppler, B. K. A comparative study of adduct formation between the anticancer ruthenium (III)

compound HInd trans-[$RuCl_4(Ind)_2$] and serum proteins. *J. of. Inorg. Biochem.* **2004**, *98*, 1135-1142.

2. Kratz, F.; Hartmann, M.; Keppler, B.; Messori, L. The binding properties of two antitumor ruthenium (III) complexes to apotransferrin. *The J. of Bio. Chem.* **1994**, *4*, 2581-2588.

3. Kratz, F.; Mulinacci, N.; Bertin, I.; Keppler, B.; Messori, L. Kinetics, spectroscopic and LPLC studies of the interactions of antitumor ruthenium (III) complexes with serum proteins. *Met. Ions Biol. Med.* **1992**, *2*, 69-74.

4. Egger, A.; Arion, V. B.; Reisner, E.; Cebrian-Losantos, B.; Shova, S.; Trettenhahn, G.; Keppler, B. K. Reactions of potent antitumor complex trans-[$Ru(III)Cl_4(indazole)_2$] with a DNA relevant nucleobase and thioethers: Insight into biological action. *Inorg. Chem.* **2005**, *44*, 122-132.

5. Jaroslav, M.; Olga, N.; Keppler, B. K. Alessio, E.; Brabec, V.; Biophysical analysis of natural, double-helical DNA modified by anticancer heterocyclic complexes of ruthenium (III) in cell-free media. *J. of Bio. Inorg. Chem.* **2001**, *6*, 435-445.

6. Brabec, V.; Novakova, O. DNA binding mode of ruthenium complexes and relationship to tumor cell toxicity. *Drug Resistance Updates*. **2006**, *9*, 111-122.

7. Chatlas, J.; Eldik, R. V.; Keppler, B. K. Spontaneous aquation reactions of a promising tumor inhibitor trans-imidazolium-

tetrachlorobis(imidazole)ruthenium(III), trans-Him[$RuCl_4(Im)_2$]. *Inorg. Chim Acta.* **1995**, *233*, 59-63.

8. Kung, A.; Pieper, T.; Wissiack, R.; Rosenberg, E.; Keppler, K. B. Hydrolysis of the tumor-inhibiting ruthenium(III) complexes HIm trans-[$RuCl_4(im)_2$] and Hind trans-[$RuCl_4(ind)_2$] investigated by means of HPCE and HPLC-MS. *J. Biol. Inorg. Chem.* **2001**, *6*, 292-299.

9. Rubin, R.; Strayer, S. D. Rubin's Pathology-Clinicopathologic foundations of medicine. 5th edition, A Lippincott Williams and Wilkins publication, **2007**, 152.

10. Price, A. S.; Wilson, M. L. Pathophysiology Clinical concepts of Disease processes. 3rd edition, A McGraw-Hill book company publication, **1986**, 102.

11. http://www.cancer.gov/cancertopics/what-is-cancer, 09/23/07, 4.30 pm.

12. http://www.cancer.org/docroot/CRI/content/CRI_2_4_1x_What_Is_Cancer.asp?sitearea= , 09/23/07, 4.40pm.

13. Kozelka, J.; Legendre, F.; Reeder, F.; Chottard, J. C. Kinetic aspects of interactions between DNA and platinum complexes. *Co. Chem. Rev.* **1999**, *190-192*, 61-82.

14. Fichtinger-Schepman, A.; Lohman, P. H.; Reedijk, J. Detection and quantification of adducts formed upon interaction of diamminedichloroplatinum (II) with DNA by anion-exchange chromatography after enzymatic degradation. *Nuc. Ac. Res.* ***1982***, *10*, 5345-5356.

15. Eastman, A. Reevaluation of interaction of cis-dichloro(ethylenediamine)platinum (II) with DNA. *Biochemistry.* **1986**, *25*, 3912-3915.

16. Lohman, P.H.; Reedijk, J. Fichtunger-Schepman, A. M.; Van der Veer, J. L.; Den hartog, J. H. Adducts of the antitumor drug cis-diamminedichloroplatinum (II), with DNA: formation, identification, and quantitation. *Biochemistry*. **1985**, *24*, 707-713.

17. Hay, W. R.; Miller, S. Reactions of platinum (II) anticancer drugs. Kinetics of cis-diammine (cyclobutane-1, 1-dicarboxylato) platinum (II) "Carboplatin". *Polyhedron*. **1998**, *17*, 2337 2343.

18. Chabner, A. B.; Longo, L. D. Cancer Chemotherapy and Biotherapy-Principles and Practice. 3rd edition, A Lippincott Williams and Wilkins publication, **2001**, 185-239.

19. Kostova, I. Ruthenium Complexes as Anticancer Agents. *Cur. Med. Chem.* **2006**, *13*, 1085-1107.

20. Zeller, W. J.; Fruehauf, D. New platinum, titanium, and ruthenium complexes with different patterns of DNA damage in rat ovarian tumor cells. *Cancer Research.* **1991**, *51*, 2943-2948.

21. Alessio, E.; Balducci, G.; Lutman, A.; Mestroni, G.; Calligaris, M.; Attia, W. M. Synthesis and characterization of two new classes of ruthenium (III)-sulfoxide complexes with nitrogen donor ligands (L). *Inorg. Chim. Acta.* **1993**, *203*, 205-217.

22. Novakova, O.; Kasparkova, J.; Vrana, O.; Van Vliet, P. M.; Reedijk, J.; Brabec, V. Correlation between cytotoxicity and DNA binding of polypyridyl ruthenium complexes. *Biochemistry*. **1995**, *34*, 12369-12378.

23. Miller, S. E.; House, D. A. The hydrolysis products of cis-dichlorodiammineplatinum (II). The kinetics of formation and anation of the cis-diamminedi(aqua)platinum(II) cation. *Inorg. Chim. Acta.* **1989**, *166*, 189-197.

24. Miller, S. House, D. A. The hydrolysis products of cis-dichlorodiamineplatinum (II). Hydrolysis kinetics at physiologica pH. *Inorg. Chim. Acta*. **1990**, *173*, 53-60.

25. Skoog, A. D.; Holler, F.J.; Crouch, R.S.; Principles of Instrumental Analysis. 6th edition, A Thomson Brooks/Cole publication, **2007**, 336-362.

26. Bouma, M.; Nuijen, B.; Jansen, M. T.; Sava, G.; Flaibani, A.; Bult, A.; Beijnen, J. H. A Kinetic study of the chemical stability of the antimetastatic ruthenium complex NAMI-A. *Intl. J. of Pharmaceutics*. **2002**, *248*, 239-246.

27. Bacac, M.; Hotze, A. C. G.; Schilden, K.; Haasnoot, J. G.; Pacor, S.; Alessio, E.; Sava, G.; Reedijk, J. The hydrolysis of the anti-cancer ruthenium complex NAMI-A affects its DNA binding and antimetastatic activity: an NMR evaluation. *J. of Inorg. Biochem.* **2004**, *98*, 402-412.

28. Bouma, M.; Nuijen, B.; Jansen, M. T.; Sava, G.; Bult, A.; Beijnen, J. H. Photostability profiles of the experimental antimetastatic ruthenium complex NAMI-A. *J. of Pharm. And Biomed. Anal.* **2002**, *30*, 1287-1296.

29. Chen, J.; Chen, L.; Liao, S.; Zheng, K.; Ji, L. A Theoritical study on the hydrolysis process of the Antimetastatic Ruthenium (III) complex NAMI-A. *J. Phys. Chem. B.* **2007**, *111*, 7862-7869.

30. Mura, P.; Piccioli, F.; Gabbiani, C.; Camalli, M.; Messori, L. Structure-Function Relationships within Keppler-Type Antitumor, Ruthenium (III) Complexes: the case of 2-Aminothiazolium [trans-tetrachlorobis (2-aminothiazole) ruthenate (III)]. *Inorg. Chem.* **2005**, *44*, 4897-4899.

31. Iengo, E,; Mestroni, G.; Geremia, S.; Calligaris, M.; Alessio, E. Novel ruthenium(III) dimmers Na2[{trans-RuCl4(Me2SO-S)}2] and [{mer, cis-RuCl3(Me2SO-S)(me2SO-O)}2] closely related to the antimetastatic complex Na[trans-RuCl4(Me2SO-S)(Him)]. *Inorganic Chemistry.* **1999**, *19*, 3361-3371.

32. Reisner, E.; Arion, V.; Guedes da Silva, M.; Fatima, C.; lichtenecker, R.; Eichinger, A.; Keppler, B. K.; Pombeiro, A. J. L. Tuning of redox potentials for the design of ruthenium anticancer drugs- an electrochemical study of [trans-RuCl4L(DMSO)] and [trans-RuCl4L2]- complexes, where L=Imidazole, Indazole,1,2,4-triazole. *Inorganic Chemistry.* **2004**, *43*, 7083-7093.

33. Mura, P.; Camalli, M.; Messori, L.; Piccioli, F.; Zanello, P.; Corsini, M. Synthesis, Structural Characterization , Solution Chemistry, and Preliminary Biological Studies of the Ruthenium (III) Complexes [TzH][trans-RuCl4$(Tz)_2$] and [TzH][trans-$RuCl_4$(DMSO)(Tz)].(DMSO), the Thiazole Analogues of Antitumor ICR and NAMI-A. *Inorg. Chem.* **2004**, *43*, 3863-3870.

34. Vilchez, F. G.; Vilaplana, R.; Blasco, G.; Messori, L. Solution studies of the antitumor complex dichloro 1,2-propylendiaminetetraacetate ruthenium (III) and of its interactions with proteins. *J. of Inorg. Biochem.* **1998**, *71*, 45-51.

35. Keppler, B. K.; Hartmann, M. New Tumor-Inhibiting Metal Complexes. Chemistry and Antitumor Properties. *Metal-Based Drugs.* **1994**, *1*, 145-149.

36. Keppler, B. K.; Henn, M.; Juhl, U. M.; Berger, M. R.; Niebel, R.; Wagner, F. E. New ruthenium complexes for the treatment of cancer. *Prog. In Clin. Biochem. And Med.* **1989**, *10*, 41-69.

37. Messori, L.; Orioli, P.; Vullo, D.; Alessio, E.; Iengo, E. A Spectroscopic study of the reaction of NAMI, a novel ruthenium (III) anti-neoplastic complex, with bovine serum albumin. *Eur. J. Biochem.* **2000**, *267*, 1206-1213.

38. Messori, L.; Kratz, F.; Alessio, E. The interaction of the antitumor complexes Na [trans-RuCl4 (DMSO) (Im)] and Na [trans-RuCl4 (DMSO) (Ind)] with apotransferrin: a spectroscopic study. *Metal-Based Drugs.* **1996**, *3*, 1-63.

39. Pieper, T.; Peti, W.; Keppler, B. K. Solvolysis of the Tumor-inhibiting Ru(III) complex trans-tetrachlorobis(Indazole)Ruthenate(III). *Metal-Based Drugs.* **2000**, *7*, 225-232.

40. Keppler, B. K.; Rupp, W.; Juhl, U.M.; Endres, H.; Niebl, R.; Balzer, W. Synthesis, Molecular structure, and Tumor-Inhibiting properties of Imidazolium trans-Bis(imidazole)tetrachlororuthenate (III) and Its Methyl-Substituted Derivatives. *Inorg.Chem.* **1987**, *26*, 4366-4370.

41. Lipponer, K. G.; Vogel, E.; Keppler, B. K. Synthesis, Characterization and Solution Chemistry of trans-Indazoliumtetrachlorobis(Indazole)ruthenate (III), A New Anti-Cancer Ruthenium complex. IR, UV, NMR, HPLC Investigations and Anti-tumor activity. Crystal Structures of trans-1-methyl-indazoliumtetrachlorobis-(1-methylindazole) ruthenate(III) and its Hydrolysis product trans-Monoaquatrichlorobis-(1-methylindazole)-ruthenate(III). *Metal-Based Drugs*, **1996**, *3*, 243-260.

42. Laidler, K. J.; Meiser, J. H.; Sanctuary, C. B.; *Physical Chemistry*, *fourth edition*, Houghton Mifflin Company, **2003**, 368-378.

43. Mc Quarrie, A. D.; Simon, D. J. *Physical Chemistry*, University science books, **1997**, 1188-1198.